CIRED ONLINE

20-23 SEPTEMBER 2021

SPECIAL REPORT - SESSION 2

POWER QUALITY AND ELECTROMAGNETIC COMPATIBILITY

Chairperson Britta HEIMBACH
Switzerland
britta.heimbach@ewz.ch

Special Rapporteur Jan MEYER
Germany
jan.meyer@tu-dresden.de

Special Rapporteur Jan DESMET
Belgium
janj.desmet@ugent.be

Special Rapporteur Herwig RENNER
Austria
herwig.renner@tugraz.at

Introduction

The **scope of Session 2** has been defined by the Session Advisory Group and the Technical Committee as power quality (PQ) including the general concept of electromagnetic compatibility (EMC) as well as related safety problems in electricity distribution systems.

Special focus is put on the impact of new technologies on voltage quality (voltage level, flicker, unbalance and distortion). This session will also look into PQ system monitoring and mitigation methods, electromagnetic compatibility, electromagnetic interferences as well as electric and magnetic fields issues. Finally, this session discusses PQ related activities in standardization and regulation.

The aim of this special report is to present a summary of the present concerns in PQ and EMC, based on all selected papers of Session 2 (99 papers). The report is divided in the following four blocks:

Block 1: Magnetic fields, grounding, safety and immunity
Block 2: Power quality issues of new technologies
Block 3: Power quality measurement, analysis and mitigation methods
Block 4: Standardization, system monitoring, handling big data and regulatory issues

An unambiguous allocation of the papers is not always possible and topical overlapping may appear to some extent between the blocks.

Three **Round Tables** are organised within Session 2:

RT15: Impact of Renewable Energy Systems (RES) and Storage on Power Quality
This round table will give an overview concerning nowadays challenges in solving PQ related issues due to the massive integration of renewables and storage systems.

RT17: Emission Limits and Assessment of Disturbing Customer Installations
The calculation of emission limits for customer installations and techniques to evaluate the compliance of a customer installation with given limits are in the focus of this round table. Their importance and practical applicability are discussed from different viewpoints.

RT19: The Future of Flicker
The aim of this round table is to discuss possible options how to deal with flicker in the future. They might include new methods for flicker measurement, relaxed limits as well as abandoning “flicker” and replacement by “rapid voltage changes”.

The **Research and Innovation Forum** is dedicated to the impact of instrument transformers on the accuracy of distortion measurements with main focus on MV systems.

Block 1: “Magnetic fields, grounding, safety and immunity”

Magnetic Fields

In this year’s conference, three papers were addressing magnetic field issues.

The authors of [B1-0238(IT)] the mitigation of the magnetic field generated by current limiting reactors is analysed with 3D-FEM-simulations. The MF levels in the vicinity of these elements can be high enough to overcome the limits to protect both workers and the public from exposure. Different magnetic shielding configurations are analysed. From the results it can be concluded that the use of three-layered shields composed by Al+FEGO+Al can provide good results. In the optimum configuration, shielding plates are installed at the surrounding walls and partly on the floor. A shielding factor higher than 10 is achieved above 0.5 m height, while a lower efficiency is observed in the lower area.

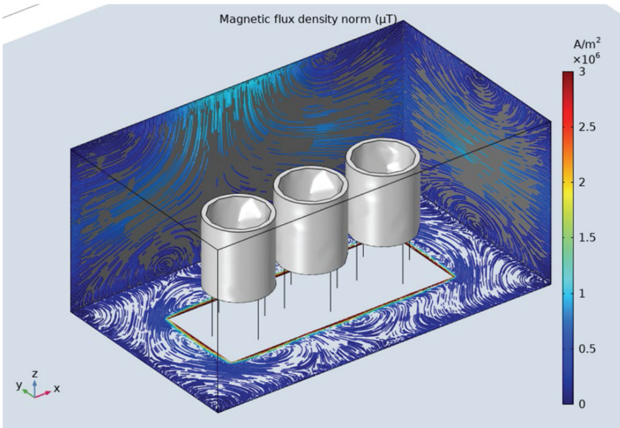

Fig. B1-1: Current density streamlines inside the inner Al shield for the solution with partly covered floor [B1-0238(IT)]

The use of an innovative magnetic field source for the practical testing of low-frequency magnetic shielding is presented in [B1-0736(IT)]. The proposed source is composed of three coils for the generation of rotational magnetic fields in space. The supply system is based on a signal generator that controls a power amplifier. This allows to generate an arbitrary waveform or to control the frequency of sinusoidal currents. The supporting structure of the coil system is printed with a 3D-printer. With the designed setup, a field intensity of 35 μT is achieved in a distance of 20 cm of the source. The source has been applied successfully during the test procedure of a sample plate for determining the shielding factor.

Field mitigation by use of a passive loop is analysed by the authors of [B1-1057(EG)]. The goal is to reduce the field of overhead lines. A setup with a passive loop below a medium voltage line with flat conductor configuration was chosen. The passive loop with an aluminium/steel-conductor with 150/25 mm² cross section is installed in half the height of the overhead line. Simulation show that the field is reduced by almost 90 %. However, there is no information in the paper, at which location this reduction is achieved.

Grounding systems and safety

The design, analysis and optimisation of grounding systems and earthing impedance is presented in several research papers.

The knowledge of the characteristics of soil is essential for an adequate design. Current methods for determining soil parameters are often based on assumptions of a homogeneous or simple 2-layer structure. Paper [B1-0632(AT)] compares different standardised methods as given in IEEE Std. 80 for estimating soil resistivity of a synthetic soil model. The basic idea is to find the correct soil model based on earth potential measurement data and solving this inverse problem. Best results are achieved with earth resistivity tomography (ERT) and applying an inversion model. For ERT a defined number of equidistant electrodes are placed on the soil and the measurement unit switches the electrodes automatically in a way that the maximum possible combination within the measurement array is reached. This method is already widely used in geophysical applications for ground exploration but is rather unknown in power system applications. As indicators for the comparison, earth surface potential and step voltage are used. For a more general understanding the setup of the electrodes and variation of the inhomogeneity have to be investigated.

Special short circuit tests that were performed by the authors of [B1-0258(DE)] in a medium voltage grid revealed significantly lower earthing resistance compared with standard measurement methods. It can be assumed that the current injection method shows higher values due to divergent current distribution models compared to the real earth fault. The fall-of potential method shows even larger deviations. Based on the consideration that the elements of the lattice network, representing the earthing system, are to be regarded as ohmic-inductive impedances and that today's measuring devices operate at frequencies above 50 Hz, one explanation could be found. Furthermore, there are hardly any empirical values for reduction factors available, describing the fault current distribution. This is especially valid for inhomogeneous grids with different cable types. For the verification of the results for the reduction factor as well as for the investigation of the earthing impedance measurements for different earthing conditions, further tests with real earth faults should be carried out in the future.

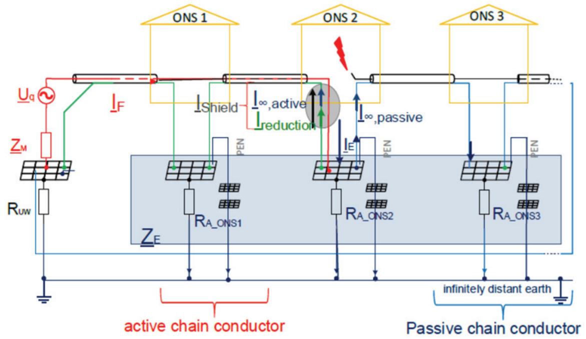

Fig. B1-2: Extended model of EN 50522 [B1-0258(DE)]

The problem of reduction factor respectively the of supplementary return paths for the ground return current is also addressed in [B1-0371(UK)]. It has been confirmed that if a supplementary metallic return path is present between the substations undergoing a fault, a reduction of the ground return current may be applied, having a significant effect upon the calculated earth potential rise. However, it strongly depends on the cable type. For plastic cables, it can be seen that with a higher soil resistivity or a smaller cable length, the ground return current would decrease. With regards to older hessian served lead-sheathed cables, the ground return current is largely related to the soil resistivity. As soil resistivity increases, the ground return current is smallest for longer cable lengths. To a lesser extent, the ground return current also depends upon the size of the cable sheath. No clear worst-case assumption can be applied for a lead sheath cable connection; therefore it is recommended that a more detailed study is conducted to calculate the ground return current in these cases.

Measurements of positive- and zero-sequence impedance in LV networks were performed by the authors of [B1-0884(DE)] by switching a load resistance and evaluating voltage and current changes. Nine LV grids were selected, covering TT and TN-C-S networks as well as a good mixture of rural, village and suburban class networks. The results for the positive-sequence impedance match the expected values, derived from typical cable parameters, with some deviations that could be explained. However, for the zero-sequence impedance the situation is different. Even accurate calculations considering the earth current depth showed larger deviations from measurement results regarding the reactance.

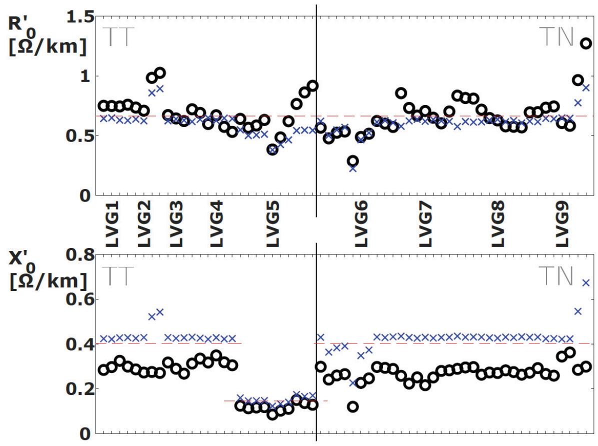

Fig. B1-3: Zero-sequence resistance (top) and reactance (bottom) per unit length of all cable sections evaluated, (left) TT network measurements, (right) TN network measurements, red (dashed) line indicating typical cable parameters, blue crosses as calculated values with respect to earth current depth [B1-0884(DE)]

For substations with high fault levels it can be very demanding to design adequate earthing systems, if only traditional techniques are used. Additionally, small footprint area, which limits the earthing grid area, high resistivity soils, and poor reduction factor may ultimately lead to almost unfeasible and expensive earthing system designs, comprising dozens of long vertical electrodes. To overcome those problems, a novel design is introduced in paper [B1-0838(PT)]. The new design is based on the installation of an electro-welded steel mesh reinforced pavement, connected to the earthing grid, and the use of plastic insulated fences with a known breakdown voltage (approximately 4 kV). The touch voltages in the areas with the steel mesh are extremely low, as can be seen in Fig. B1-4. Regarding the switching station fence, the expected maximum touch voltage is 3500 V at the corners, still 700 V lower than the lowest breakdown measured voltage, thus, the safety of people is guaranteed in this solution. Compared with traditional design, a significant reduction of costs is achieved.

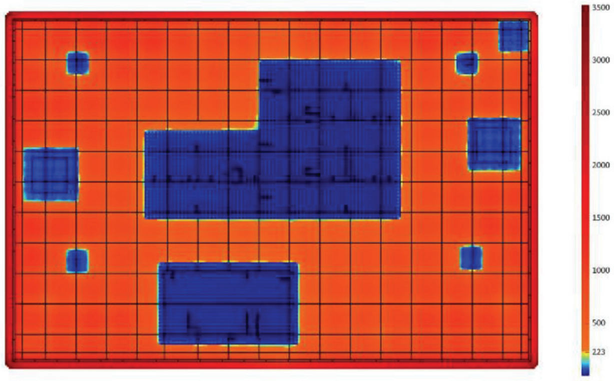

Fig. B1-4: Touch voltages results for the novel earthing grid design solution – red: unsafe areas, except for the insulated fence, blue: safe with steel mesh reinforced pavement [B1-0838(PT)]

Decentralized earth fault compensation coils (EFCC) in resonantly grounded medium-voltage networks are becoming increasingly popular. Their installation places several demands on the earthing system with regard to equipment and personal safety. In [B1-0969(AT)] the authors analyse two MV grids, representative for an urban and a rural area. The effective earthing impedance and thus the earth potential rise is mainly determined by the (global) earthing systems. Another issue is the current distribution during an earth fault. Especially the cable shields of cables connecting ring main units with EFCC are affected.

In the Brazilian distribution grids, primary consumers or loads may be connected between the MV phases and the neutral conductor. In these situations, the neutral used in the MV is the same for the LV loads, called a common neutral conductor. Breakage of the common neutral and its consequences – overvoltage, undervoltage, voltage imbalance - is analysed in [B1-0197(BR)]. The phenomena strongly depend on the type of distribution transformer, grounding resistance and load. Simulation of a representative distribution grid were performed. Overvoltage as a consequence of neutral MV breakage only occurs in very poor grounding and imbalance conditions. In the LV system, phase-to-neutral overvoltage up to 2 pu were observed.

Safety and Immunity

Residual current devices (RCD) are important for ensuring personal safety and protecting from electric shock in case of insulation failures. Reliable tripping as well as avoidance of undesired malfunction is essential. The authors of [B1-0060(SE)] studied the impact of quasi-dc (0 - 4 Hz) and supraharmonics on the tripping characteristics of different types of RCDs with the aim to identify fail-to-trip and false tripping conditions. There is a clear gap in standardization regarding the frequency components included in test signals. Presence of supraharmonics might cause that higher 50 Hz currents are needed for the RCDs to trip. Fail-to-trip situations have been identified for residual currents with frequencies other than 50 Hz. AC-type RCDs should be avoided in cases of half wave pulsating residual currents with and without superimposed distortion since they failed to trip.

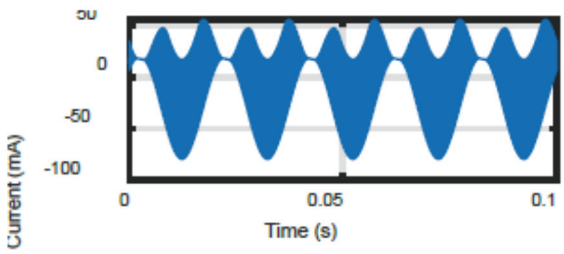

Fig. B1-5: Test residual current, half-wave pulsating, 50 Hz and supraharmonics [B1-0060(SE)]

In the modern grid different types of voltage disturbances in the power supply are expected due to the integration of renewable energy sources and electric vehicles. These voltage disturbances affect the luminaires lifetime and may lead to light flicker and failures of LED lamps. In [B1-0026(SE)] a literature review on LED life assessment by accelerated test methods is done. LED driver circuits are responsible for about 60 % of failures. Cost-effective solid-state driver circuits or driverless topologies capable of handling adverse stress conditions need to be developed. Appropriate accelerated tests with stochastic input such as fast voltage fluctuation due to EV charging, undervoltage and overvoltage due to EV and PV interactions etc. need to be developed for LED lifetime estimation.

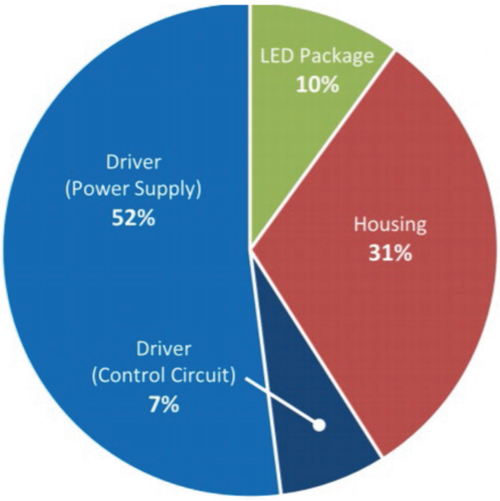

Fig. B1-6 Distribution of LED failures (Source: Appalachian Lighting Systems, Inc.) [B1-0026(SE)]

Potential scope of discussion

There are still a lot of uncertainties in the field of grounding system engineering. Simplified assumptions about the soil characteristics are used, which might lead to expensive earthing designs to guarantee safety. In addition, the impact of global earthing systems has to be further investigated.

Table 1: Overview of papers in Block 1

Paper (No. and Title)		MS	RIF	PS
0026	LED Life Assessment by Accelerated Test Methods – a Review			I
0060	Impact of Supraharmonics and Quasi-DC on the Operation of Residual Current Devices	X		
0197	Overvoltage Analysis in Low Voltage Consumers Caused by Neutral Conductor Opening in the Power Distribution Grid			X
0238	3D Shielding Modelling and Design of Three Phase Current Limiting Reactances			X
0258	Interpretation of Reduction Factor and Earthing Impedance According to EN 50522 Through Earth Fault Tests in a Medium-Voltage Grid with Low-Impedance Neutral Earthing	X		
0371	Effect of a Supplementary Return Path on Ground Return Current	X		
0632	Earth Resistivity Tomography for Earthing System Design	X		
0736	A Proposal for Performance Evaluation of Low Frequency Shielding Efficiency			X
0838	Application of a Novel Cost-Effective Earthing Design Solution for Switching Stations with High Short-Circuit Power, Using an Integrated Methodology	X		
0884	Determination of Positive- and Zero-Sequence Components of Line Sections in Low-Voltage Networks Using Impedance Measurements	X		
0969	Decentralized Earth Fault Compensation in MV-Grids – Challenges and Solutions			I
1057	Passive Loop Mathematical Model as a Reduction Method for Overhead Line Magnetic Field			X

I: interactive poster presentation

<u>Block 2: “Power quality issues of new technologies”</u>

Photovoltaic

In paper [B2–0013(SE)] the peak load balancing of PV by integration of EV with respect to its challenges like multiple converter interactions leading to grid instability issues, voltage distortion and variations, resonances etc. are discussed. Especially the parallel operation of multiple converters and the impact on stability in a low voltage DC system integrating EV, PV and a grid connected rectifier are investigated in a theoretical way from the rectifier perspective. The system stability was investigated with parallel operation of multiple converters and their control systems. The most critical component that can ensure stability is identified as the substation rectifier DC-link capacitance since it will enhance damping of a low frequency enabled stable operation. From simulations, it was identified that the voltage mode control operation is more robust compared to the current mode control in the studied interconnected system.

Paper [B2–0285(EG)] studies the characteristics of low order harmonics emission from 18 installed small-scale PV (SSPV) systems with different capacities and different inverters type. According to the Egyptian grid code for small-scale PV, the PV system output should have low current distortion levels to ensure that no adverse effects are caused to other equipment connected to the utility system. The results of the survey of harmonic emission level from these small scale solar inverters are presented. It is concluded that the total harmonic distortion of the current almost exceeded the maximum permissible limit of 5% due to active power injected by the PV inverters, which varies due to different conditions. Concerning supraharmonic emission in the range 2 kHz – 9 kHz, the dominant harmonic current was found at 2.7 kHz.

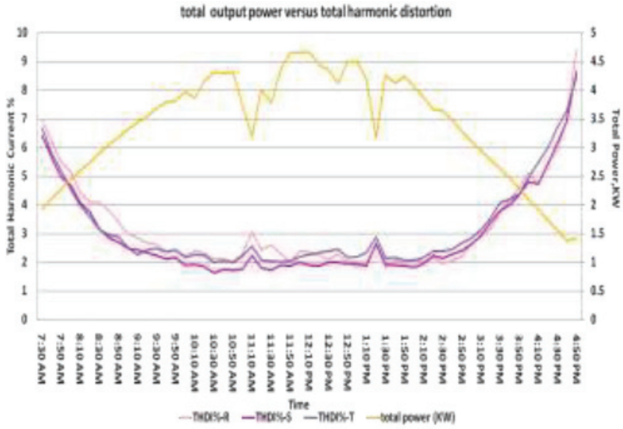

Fig. B2-1: Total output power versus total harmonic current distortion emitted from the SSPV for site at the same time [B2–0285(EG)]

A methodology to regulate power factor in installations with solar self-consumption is discussed in [B2–0891(FR)]. Photovoltaic energy is a strongly emerging technology and excellent as sustainable energy source. Despite all benefits, PV installations may lead to power factor degradation. To avoid this degradation, an algorithm-based solution for PV inverters is presented. The purpose of the presented method is to define in real-time the optimal set points of the photovoltaic system to avoid excess reactive power charges, but also to maximize the active power input from the photovoltaic inverters, so that the end user can get the maximum from its local energy production system. The proposed method is purely based on analytics and do not require loop control systems. It allows to fix the power factor at the point of common coupling with high accuracy while maximizing the active power and injecting a minimum of reactive energy. It can be concluded that the proposed approach is cost-effective and does not require the installation of additional equipment for power factor correction but economic benefits should be evaluated case by case.

Wind

It is common knowledge that wind-power installations influence the waveform distortion in the surrounding network. Details and the challenges to avoid waveform distortion however are less well known. The contribution [B2–0028(SE)] summarizes the results from four consecutive projects with respect to the waveform distortion in and around wind-power installations. It is highlighted that high levels may occur due to a number of reasons, since harmonics and wind-power installations are a complicated issue and it is still not possible to predict when and where high levels will occur. However, it can be concluded that harmonics are not a major issue with wind-power installations. High levels of harmonic currents or voltages occur rarely and there is no need for strict requirements on each individual installation. A building up of general knowledge on this subject and monitoring levels and trends are of major importance, since modelling challenges and simulation are at this moment no obvious solution.

Paper [B2–0184(SE)] verifies the fault-ride-through of wind turbines using two distinct characterization approaches to obtain synthetic dip profiles based on real measurements. The first approach is based on the CIGRE checklist, while the other approach considers only magnitude and duration as characteristics of the voltage dip. The aim of this comparison is based on the fact that most of the fault ride through studies do not consider the latter in their evaluation. The verification is done in a Swedish wind park on double-fed-induction-generator (DFIG) turbines. The result of this study shows that by considering the detailed characteristics of the voltage dip a lower difference in the dynamic behaviour compared to the simplified synthetic profile is obtained, since the simplified synthetic profile shows overestimation as well as underestimation of the dynamic behaviour during all the stages of the voltage dip.

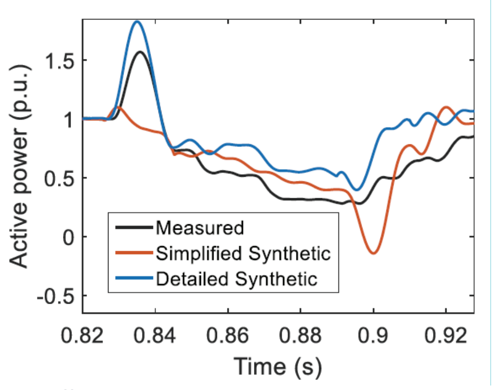

Fig. B2-2: Difference in active power between measured, simplified and detailed synthetic dip profile [B2–0184(SE)]

[B2–0389(UK)] develops and validates an equivalent model of a wind farm for probabilistic harmonic propagation and mitigation studies in power electronics rich transmission or distribution networks. The used methodology is based on both probabilistic distributions and Monte Carlo simulations and is validated by measurements from a single wind turbine. Using a single probabilistic harmonic generator and commercial software package for power system analysis, this paper proposes appropriate modelling ranges and distributions of the equivalent model parameters and then validates the equivalent model of the wind farm based on field measurements at the PCC bus. It is concluded that the simulation results using the developed model reflect a good estimation of the available field measurements. This equivalent model is therefore deemed to be suitable for the first level approximation of harmonic propagation and the identification of potential harmonic issues in power electronics rich networks.

Battery storage

Paper [B2–0263(UK)] analysis the possibilities for mitigating the voltage unbalance in rural low voltage networks using single-phase BESS inverters. Therefore single-phase load demands are modelled using real consumption data on 1-minute-basis, while voltage unbalance is quantified corresponding the IEC 61000-2-2 standard. The BESS units are modelled in detail including the main electrical components and the control system. It is assumed that the BESS inverters can deliver both active and reactive power in order to limit the unbalance in the network with respect to overload conditions. The used distribution network model is based on a German rural network and consists of 24 customers connected via cables and overhead lines to the distribution transformer. Unbalance is quantified as negative–sequence to positive-sequence voltage ratio. A 24-hour simulation is carried out to identify the hour with the highest voltage unbalance levels and subsequently a sensitivity analysis is carried out to investigate the impact of installing the BESS at different locations in the distribution system. The results of this analysis show that single-phase BESS units can effectively mitigate voltage unbalance in residential distribution networks.

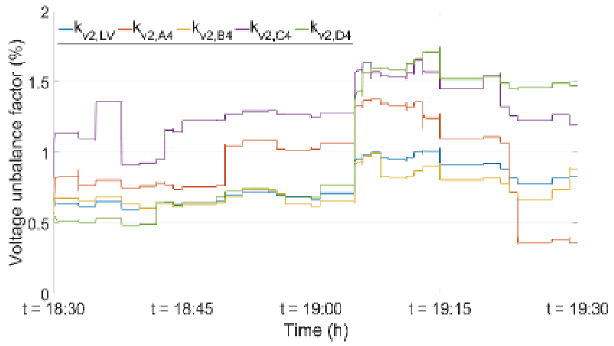

Fig. B2-3: Voltage unbalance factor without local storage [B2–0263(UK)]

Electric vehicles

Paper [B2–0202(EG)] illustrates both harmonic voltage and current distortion caused by electric bus fast battery charger while maintaining the standard limit of the IEC 61000-3-12. As it is shown, the measurements carried out at the PCC comply with the limits of IEEE 519-2014 standard. Next to that, also the frequency range of the currents from 2 kHz up to 9 kHz is analysed. The charger measurements at the PCC showed compliance of the total harmonic voltage distortion with the IEEE 519-2014 standard, even so the total current demand distortion for the eight chargers and cumulative percentage P0.99 were within the standard limits. Current analysis confirmed the typical 5th and 7th order harmonic, however the 7th was the dominant one. Analysing the impact of higher frequency components a maximum was found at frequency of 2.1 kHz but also a component at 5.1 kHz was observed.

The impact of fast-charging of electric buses on the power quality based on field measurement in the Netherlands is discussed in [B2–0252(NL)]. A pilot study has been performed in a major city of the Netherlands, where every day many fast and slow charging of electric buses takes place in the same bus depot, which can be considered as point of common connection. Since EV chargers are basically power electronic converters they are sources of both harmonics and supraharmonics. Power quality analysis is performed in PCC and various PQ measurement results are summarized and discussed. Concerning low frequency disturbances such as harmonics, voltage variations and flicker, all parameters are within the limits of the EN50160. In addition, supraharmonics who can create problems at specific frequencies especially in case of end users consumers gave no significant impact.

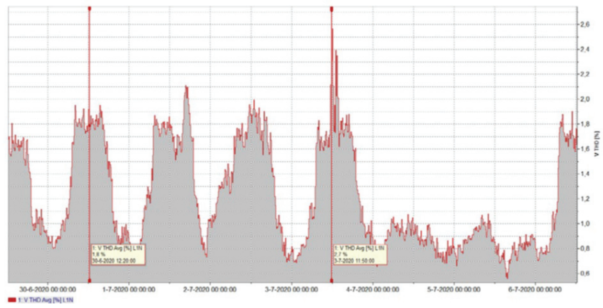

Fig. B2-4: Weekly profile of total harmonic voltage distortion at a fast charger terminal [B2–0252(NL)]

In paper [B2–0473(FR)] the results of a study carried out for a depot with a capacity of 200 electric buses are compared in terms of different electric distribution architectures and the equipment making up these infrastructures. An overview of centralized and distributed solutions both in DC and AC were analysed. Out of the detailed analysis of the bus depot it is concluded that a centralized architecture distributing DC voltage, using 12-pulse rectifiers gives the best compromise on both the technical and economic criteria. However, this topology has the limitation that it does not allow V2G operation, which requires active frontends based on IGBT rectifiers. The AC distribution is nowadays probably still the easiest solution to install, however, it is shown that it is the least attractive solution in terms of energy consumption and of capital expenditure costs, as it requires the purchase and installation of several cables of large sections.

The increasing number of battery electric vehicles (BEVs) and plug-in hybrid vehicles (PHEVs) in the low-voltage grid must be considered in future simulations and new grid designs. For this purpose, measurements of load profile curves of EVs are performed in order to analyse the influence on voltage quality characteristics such as unbalance, rapid voltage changes, flicker and harmonics. Paper [B2-0503(GE)] describes and discusses load profile curves of 13 electric vehicles of different brand and associated PQ parameters. For the majority of the EVs, a very shortened constant voltage phase of a few minutes (from max. power to zero) is measured. For two charging cycles the maximum unbalance limit due to VDE AR-N 4100 is exceeded. The effects of the EVs on voltage quality vary significantly between the different vehicle types.

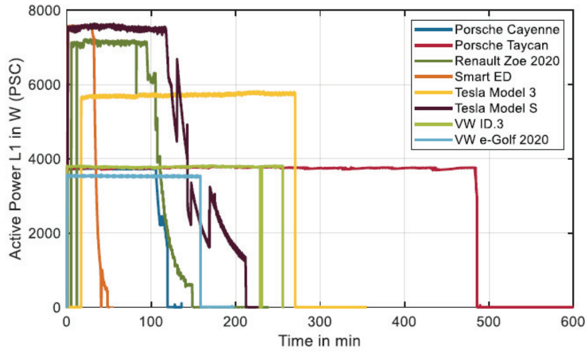

Fig. B2-5: load profiles of 2 phase and 3-phase charging EVs in active power [B2-0503(GE)]

In paper [B2–0835(GE)] the challenges for the distribution network operators due to the increasing penetration of battery electric vehicles on PQ issues in public low voltage networks is discussed. It is shown that the changes in boundary conditions for network planning in LV networks is affected. The high coincidence of charging of multiple vehicles, mostly in the evening, can create unusual high demand situations, especially due to the fact that many EVs are single-phase connected. As a result, an increasing voltage unbalance in the network is observed. Next to that, the power electronic based rectifiers of EVs can emit both significant harmonics and supraharmonics. Two comprehensive field studies, namely a distributed charging infrastructure with eight BEVs and a central charging infrastructure with 45 BEVs were carried out in two different public low voltage networks in Germany. It is concluded that voltage unbalance limit of customer installations should not be independent of the short circuit power at the connection point in order to improve the utilization of hosting capacity, while low order harmonic and interharmonic currents are observed.

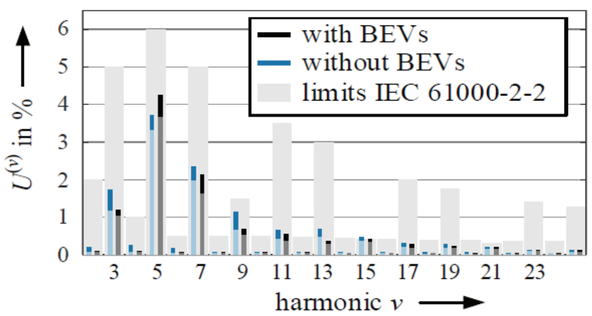

Fig. B2-6: Harmonic voltage magnitudes (95 % quantile and maximum) for long-term measurement with and without BEVs [B2-0835(GE)]

A survey of harmonic and supraharmonic emission of fast charging stations for electric vehicles in China and Germany is presented in [B2–1151(CN)]. Due to the massive integration of EVs there is the need for charging stations. Especially, in case of fast charging stations, DC chargers are used but not that much is known yet about their emission characteristic. The measurement results of 20 different chargers obtained from both China as well as in Germany are summarized and findings are discussed with focus on harmonic and supraharmonic emission up to 50 kHz. The analysis of the harmonic emission was limited to those time intervals where the highest charging currents occurred. It can be concluded that for power ratings up to 50 kW German chargers tend to have higher emission at odd harmonic orders than the Chinese chargers, while 5th and 7th harmonic current are the predominant harmonics in both countries.

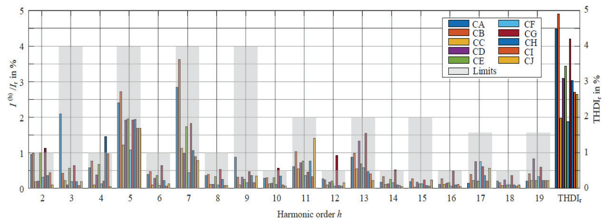

Fig. B2-7: Harmonic current emission of fast chargers in China (in % of rated current) [B2-1151(CN)]

LED lighting systems

The deviation from linear summation law for large number of homogeneous LED lamps is analysed in paper [B2–0072(SE)], where high energy LED lamps are studies with the aim to quantify the deviation of a linear increase from both harmonic deviation factor and aggregation exponent perspective in the frequency range up to 2 kHz. Therefore, measurements are performed in an installation with lamps of the same brand and type. After warming up, both current and voltage waveforms are recorded for each measurement and the harmonic spectra are obtained using DFT in Matlab, where each individual harmonic order is obtained as a function of number of lamps. It is experimentally shown that for large number of homogenous LED lamps aggregation can lead to both underestimation and overestimation of aggregated harmonic emissions. This is valid for all harmonic orders. Since the lamps are not exactly the same, the differences between individual lamps generally increase with harmonic order. In general, however for same

LED lamps the linear summation law will give reasonable results.

Increased harmonic emission challenges nowadays equipment function especially in case of LED lamps, e.g. by causing undesired light intensity variation. Paper [B2–0461(SE)] studies this phenomenon deeper by analysing the harmonic impacts on LED drivers. Therefore, experimental studies are carried out where instantaneous light intensity, average light intensity, DC-link voltage and modulation depth, are investigated for different harmonic magnitudes, phase angle and harmonic orders. For testing of LED drive circuits, 1 %, 3 %, 5 % and 7 % individual voltage harmonics from 5^{th} to 11^{th} are applied. Results show that the existence of harmonics results in deviations in the light intensity depending on the phase angle and harmonic magnitude. This indicates that the sudden changes in harmonics can lead to variation in the average light intensity. If this variation is in the range of human visibility sensation, it results in temporary light flicker.

LED lamps with a power rating greater than 5 W need to fulfil the requirements as described in e.g. IEC 61000-3-2, EN 62612 and IEC 61000-4-13. Standardized test conditions can deviate from real environments and real grid conditions and a distorted grid voltage can significantly change the magnitude of the harmonics being injected by non-linear loads. The paper [B2-0077(SE)] discusses, how the term aging process in LED lamps affects the harmonic emission and how voltage distortion can affect the aging process. A total of 1080 LED lamps are being subjected to six different voltage profiles, going from undistorted grid over background distortion and voltage variations during 6500 hours while their performance in terms of current quality has being monitored. Even if the groups consist of identical lamps, there is a difference in the harmonic profile between the different setups, which is most pronounced for the higher order harmonics. It can be concluded that long-term aging seems to have a decreasing effect on the harmonic emission from LED lamps. However, the background voltage profile is seen to have an impact on the current harmonic emission, which is well known. The LEDs directly fed from the grid showed the largest decrease in current THD.

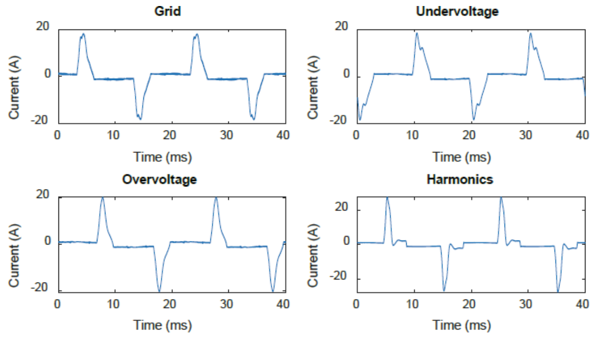

Fig. B2-8: Current waveform for four identical groups of lamps fed by different voltage profiles [B2-0077(SE)]

Further aspects

Paper [B2–0048(SE)] discusses interharmonics under fundamental frequency variations due to sustainable, new technologies. Different interharmonic patterns are observed in a number of sustainable energy sources and loads with respect to the signal processing of interharmonics of non-stationary signals. They are evaluated especially from the viewpoint, if these are real or just created by signal processing error and consequently misinterpreted as interharmonics. Case studies are performed on a wind farm, a PV inverter and a single-phase AC EV charger. Short time Fourier transform algorithm, desynchronized processing techniques and sliding-window ESPRIT are applied to the signals. From the specific case study of wind farm, it is shown that the jumps in phase angle are caused by transitions between reactive and active power and consequently are a transient phenomenon. Such events are manifested in signal processing as broad fundamental frequency deviations and subsequent interharmonics that are a product of the signal processing. As a conclusion, it is important to observe the time domain waveforms and not blindly trust the frequency domain.

In contribution [B2–0132(EG)] two fault-ride-through protection schemes for mitigating the effect of voltage to ground fault on a grid-connected double fed induction generator (DFIG) coupled to a wind turbine are examined by combining both the profiles of the stator and rotor voltages and currents and the dc link voltage and current. By relating this to the electrical torque and rotor speed, both sub and super synchronous speed are compared in order to have a better performance of the DFIG operation during unsymmetrical voltage to ground faults. It is shown, that the STATCOM connected to the DFIG stator, while a three phase external impedance is connected to the rotor circuit result in high ripples at super-synchronous operation range. Other protection schemes, such as the DVR and the UPFC are suggested to improve the machine performance at super-synchronous speed.

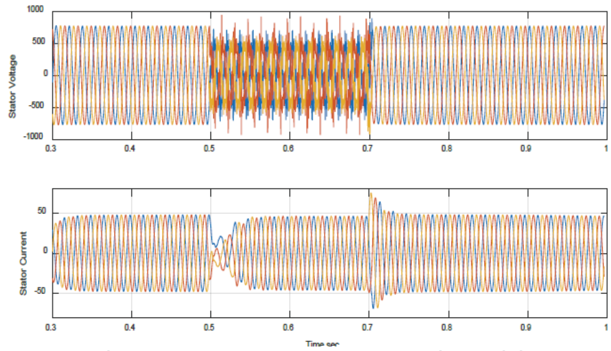

Fig. B2-9: Stator voltage and current with STATCOM and three-phase RL impedance only during faults [B2–0132(EG)]

An assessment of frequency-dependent component impedance for harmonic stability is discussed in [B2-0181(GE)] based on experimental investigations gathered out by laboratory tests using commercial single-phase inverters. It is shown, that analytical aggregation of multiple inverters at a centralized connection point is only is possible, if the individual impedances of all inverters are known and there is no mutual interaction. In the context of future standardization, type and amplitude of excitation voltages over a wide frequency range should be considered.

Paper [B2–0305(GE)] analyses the harmonic characteristics of a microgrid, which is composed of a single PV inverter, a battery charger and a number of household devices both from the type linear and non-linear. The aim of this study was to analyse different load scenarios under both interconnected and islanded operation from voltage and current harmonic distortion perspective. With the comparison between the islanded mode and interconnected operation, a detailed analysis of impact of power share between multiple power electronic generation sources is analyzed with the aim to provide a holistic perspective towards EMC coordination and standardization for islanded microgrids. It is concluded that the voltage distortion is higher in islanded operation mode than in interconnected mode due to the higher network harmonic impedance of the microgrid. Depending on the amount of non-linear loads and installed power, harmonic distortion might exceed the IEC compatibility levels.

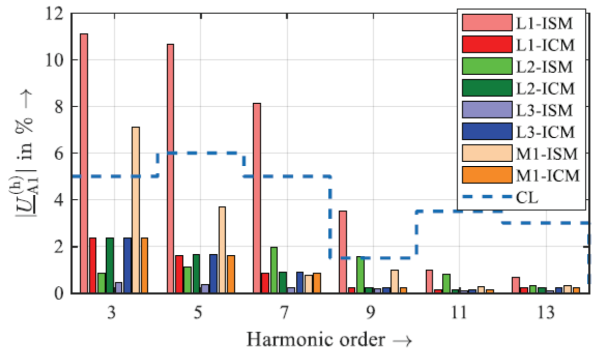

Fig. B2-10: Voltage harmonics for load scenarios measured in interconnected (ICM) and island (ISM) mode [B2–0305(GE)]

A bang-bang controller for enhanced islanded microgrid frequency stability is discussed in paper [B2 – 0379(AT)]. In contrast to distribution grids, islanded microgrids have a low inertia, especially in case of a high penetration of power electronics. Consequently, conventional frequency control has to be improved. A novel control method, including load step pre-announcement (LSP) and bang-bang (BB) controller is used to reach this goal, since frequency disturbance caused by them does not create an instability issue. A simulated islanded microgrid consisting of a conventional generator, PV infeed and a lumped load is used as a study case. The simulation results illustrate that the dynamic frequency behaviour is significantly improved using the proposed control method with optimal settings of pre-set and total time for both 25% and 50% share of PV. The performance of the proposed controllers strongly depends on pre-set and optimal time settings.

Contribution [B2–0479(SE)] discusses the future impacts on grid from both energy flow and power quality perspective based on the growing need for data centres and their power consumption. Since a data centre can consume up to 1 MW, insight on their impact in terms of power quality on the grid, especially with respect to the increased use of renewable energy sources such as wind and PV, is needed. In this paper, six sets of measurements from high voltage over medium voltage to low voltage were obtained in Sweden. Based on the analysed data, no energy deficiency has been observed in the area. However, as data centres will grow in the future and power production from renewable energy sources will increase, data centres will become more sensitive to changes in both harmonic emissions and power variations. The impact of data centres on the magnitude of aggregated harmonics at MV can lead to both a reduction or an increase in harmonic content. On its turn, higher current distortion can lead to increase in energy losses in the system, albeit the losses are rather low when compared to the power transfer losses in transmission and distribution.

The development of test methods for the investigation of the stability of inverters in low voltage grids with relation to reactive control is presented in [B2–0487(GE)] by experimental investigation of the behaviour of three inverters. The evaluation of the influence of grid impedance and the steepness of the Q(U)-relation on the control stability is investigated by analysing the difference of RMS values and the mean value of the voltage. Since the effect of the reactive power on the voltage in the network increases with increasing inductivity, an increased distance between connection point and transformer can lead to instabilities in the system. The investigated criteria show that an increased slope of the Q(U)-relation in combination with a decreased R/X-ratio may lead to problems with power quality.

Paper [B2–545(PT)] assesses the power quality of emergency generator units. Hence emergency generators and mobile power are usually not used for normal grid operating conditions, power quality related issues should still be met in order to provide optimal supply quality to the customer. Next to that, the distribution network operator must always comply with the EN 50160 standard. An analysis of different types of emergency generators and mobile power plants operated by E-REDES were assessed with respect to the compliance of the power quality standards corresponding with the NP EN 50160. Due to the short operating duration, it was not possible to fully conclude, if the supply voltage is in accordance to the NP EN 50160 standard. Although, it was possible to have an image of the overall quality of service provided by this type of assets. It was concluded that the monitored emergency generators voltage characteristic values where within the NP EN 50160 limits, even in cases where load variations were most pronounced. The overall performance of these assets was very good.

Paper [B2–0886(CZ)] is focused on the advanced design of responsive demand control into heat accumulation for energy management for prosumers. The approach is implemented in installations with a small-scale power generating unit in order to provide real equilibrium between electricity generation and consumption. Current and novel power flow control strategies are compared with regards to both power quality issues and energy measurements with standard meters. Finally, the total cost of installation are compared with respect to different topologies of power converters. From experimental results, it is shown that even though the performance might be improved using different topologies, universal devices cannot provide sufficient switching frequency and thus the cost of corrective and/or mitigating devices is still high. Specialized solutions providing sufficient switching frequency are worth to be developed in order to reduce the relative cost of compatible solutions.

Paper [B2–1106(UK)] describes techniques that have been used to pinpoint the root cause of tripping, overheating and harmonic distortion linked to solar arrays and to prevent recurrence. The techniques presented include both power quality measurements, residual & stray current measurements and earthing tests since most inverters will exhibit some degree of natural ‘leakage’. This tends to be related to the DC leakage of the system transferred across to the AC side, where standard 30mA RCDs (residual current devices) may experience nuisance tripping, particularly in wet weather. This issue is not only seen in domestic solar installations, but also in large solar arrays mainly due to leakage to earth through cabling and from PV panels to earth. A number of techniques which have been used to good effect to identify the sources of problems on solar and other generation sites are evaluated.

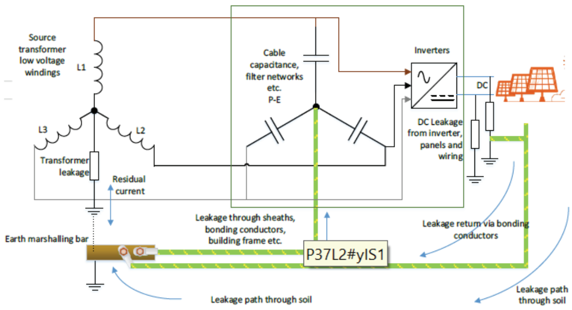

Fig. B2-11: Typical PV system showing current flow paths [B2–1106(UK)]

Potential scope of discussion

Upcoming integration of storage systems will or can reduce PQ problems in the grid, especially related to mitigation of unbalance and overvoltages caused by renewable energy sources. However, due to the upcoming grid flexibility with the aim to increase local hosting capacity, unbalance, flicker and both low and higher frequency disturbances (supraharmonics) in the grid may increase. In combination with the upcoming integration of EVs, the distribution networks will be massively affected, much more than nowadays by PV inverters. It is recommended to analyse and monitor charging stations from both stationary batteries and EVs in order to obtain sufficient information for a reliable assessment of their impact on both hosting capacity and power quality related issues.

In contrast to former CIRED conferences, the interest for the impact of wind turbines is rather low and shifted mainly to the study of massive integration of LEDs and the upcoming challenges of the integration of EVs in terms of their impact on power quality. However, renewable energy power plants still may have a significant impact on power system operation, such as voltage variations, unbalance and flicker effects. In addition, intensified monitoring and publication of results is recommended.

As mentioned before, LED technology is massively increasing in modern electricity distribution networks both in residential installations and public lighting. Due to their technology, power electronic converters are needed to control these types of lamps, creating various harmonics profiles and causing negative impacts on electrical equipment in electricity distribution networks. Future evaluations of the massive integration of this type of loads and their interaction with both linear and nonlinear loads and sources need to be monitored and followed up.

Table 2: Overview of papers in Block 2

Paper (No. and Title)		MS	RIF	PS
0013	Design and stability of a low voltage DC system integrating EV with PV			X
0028	Harmonics and wind-power installations – findings and recommendations			I
0048	Interharmonics under fundamental frequency variations	X		
0072	Deviation from linear summation law for large number of homogeneous LED lamps			X
0077	Power quality during aging of LED lamps			I
0132	Simple Scheme to Mitigate The Effect of Unsymmetrical Voltage Sag on Double Fed Induction Generator			I
0181	Experimental measurements of frequency-dependent component impedances for harmonic stability assessment			X
0184	Comparative Analysis between a Measured Voltage Dip and its Equivalent Synthetic Dip on the Dynamic Behavior of a Wind Turbine			X
0202	Harmonic Distortion Caused by Electric Bus Battery Charger in Alexandria Distribution System			X
0252	Determining the impacts of fast-charging of electric buses on the power quality based on field measurement			I
0263	Mitigation of voltage unbalance in rural low voltage networks using single-phase BESS inverters			I
0285	Survey of Harmonic Emission Level from Solar Inverters			X
0305	Waveform distortion characteristics of an islanded microgrid with residential loads	X		
0379	Optimizing load step pre-announcement and bang-bang controller for enhanced islanded microgrid frequency stability			X
0389	Validation of the Equivalent Model of Wind Farm for Probabilistic Harmonic Propagation Studies	X		
0461	Interferences in LED lamps due to Harmonic Distortion	X		
0473	How to choose the best electric network for a large electric buses depot			I
0479	Future impacts on grid: energy flow and power quality			I
0487	Development of test methods for the investigation of the stability of inverters in low voltage grids			X
0503	Measurement of the voltage quality and load profiles of electric vehicles			I
0545	Impact of high penetration of battery electric vehicles on power quality in public low voltage networks			I
0835	Impact of high penetration of battery electric vehicles on power quality in public low voltage networks	X		
0886	Advanced Design of Responsive Demand Control into Heat Accumulation for Energy Management of Prosumers			I
0891	Methodology to regulate power factor in installations with solar self-consumption.			I
1106	Advanced techniques for troubleshooting solar arrays and generator connections			X
1151	Survey of harmonic and supraharmonic emission of fast charging stations for electric vehicles in China and Germany	X		

I: interactive poster presentation

Block 3: "Power quality measurement, analysis and mitigation methods"

This block contains papers dealing with simulation-based and/or measurement-based studies dedicated to different power quality phenomena and disturbance cases. It further covers methods and devices to mitigate network disturbances. Finally, papers discussing different aspects of instrumentation and measurement are allocated to this block.

The dominating share of papers is dedicated to medium and low voltage networks. Several papers address also high voltage networks, which underlines the fact that power quality is a system issue not only limited to a certain voltage level or the distribution network.

55 % of the papers deal with simulation of harmonics (frequencies below 2 kHz) and supraharmonics (frequencies above 2 kHz), which are also referred to as higher frequency distortion. The number of papers addressing each frequency range are almost balanced. Many of those papers studying the impact of frequency-dependent impedance on interaction and propagation of distortion. Only about 11 % of the papers are dedicated to other power quality phenomena, namely flicker and sags, presenting a good diversity between simulation-based and measurement-based papers. Another 17 % of the papers are dedicated to mitigation devices and control techniques for those devices as well as one mitigation case study. The remaining 17 % of papers are almost exclusively related to the impact of the frequency-dependent transfer characteristic of instrument transformers on the accuracy of distortion measurements. As this subject seems to attract particular attention in the community, it has been decided to dedicate the RIF (research & innovation forum) exclusively to this topic.

Compared to the conference two years ago, distortion and related topics like resonances and network impedance remain important in this year's conference. Particular the number of papers addressing the frequency range 2-150 kHz has increased significantly. On the other hand, the interest in other power quality phenomena including voltage sags is not as high as at conferences before. Topics related to power quality measurement instrumentation itself almost disappeared for this year's conference. Contrary, the accurate measurement of distortion below and above 2 kHz in MV distribution networks obtained much more attention compared to former conferences.

Harmonics and interharmonics

Nine papers in Block 3 are dedicated to different aspects related to harmonics. Beside one dedicated interference case study and two papers about measurement surveys, all other papers are focused on modelling and simulation. Most of these papers look in particular on harmonic impedance, which forms the link between harmonic currents and voltages.

[B3-0748(PT)] investigates an incident, where an HV system has been tripped by an EHV/HV transformer due to elevated 5th harmonic. At the time of tripping, a second power transformer was energized in parallel, while restoring normal grid operation after reconfiguration for commissioning works. Based on an EMTP simulation it was found that a sympathetic inrush of first (tripped) transformer caused by the inrush of the second transformer resulted in a high harmonic distortion in the zero-sequence voltage component on the HV side, which in turn excited an existing zero-sequence resonance between the transformer and the extensive underground cable network. A reconfiguration of the HV network is proposed to shift the resonance between two harmonics, which can decrease the disturbance levels significantly. Furthermore, the settings of more than 6000 earth-fault protection relays has been checked to ensure that only current fundamental is used as tripping criterion.

[B3-0351(SP)] is one of two papers dealing with measurement surveys in LV networks. Odd harmonic currents up to 25th order has been measured in 15 different homes for almost one year. Besides a statistic of the homes itself in terms of size, number of inhabitants and additional information about the penetration of homes in Spain with electric appliances, the paper presents a comprehensive statistical analysis of 3rd, 5th, 7th and 9th harmonic in terms of magnitude and phase angle. Magnitude cannot be modelled by simple normal distribution, but requires more complex representation, e.g. by mixture distribution. While 3rd and 5th harmonic current clearly show a prevailing direction, the phase angle of 7th and

9th harmonic become increasingly random and wider spread. Finally, the volatility in terms of minute-to-minute transition has been analysed. Results show a dominating share of transitions being for all harmonic orders below 1 % in magnitude and 5° in phase angle.

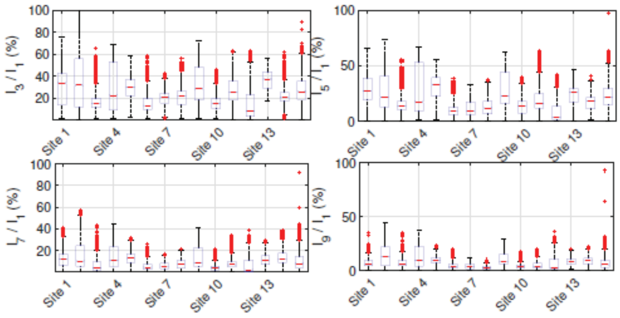

Fig. B3-1: Boxplot for harmonic current magnitudes at different measured sites [B3-0351(SP)]

[B3-0137(SE)] reports results of a measurement survey performed at the terminals of three homes, an office building and a university campus to characterize the unbalance in harmonic voltages and currents. All analyses are performed in sequence components and a definition of balanced and unbalanced THD is introduced for further discussion. The results confirm that considerable unbalance exists for all harmonic orders, as for each harmonic next to the prevailing sequence component (balanced component) also the non-prevailing sequences (unbalanced components) do exist with non-negligible magnitudes. However, the balanced components do usually dominate. An important observation is that for triplen harmonics the ratio between unbalanced and balanced components is usually higher than for the non-triplen ones. This is valuable input, i.e. for further discussions about calculating current emission limits for LV installations.

[B3-0440(DK)] proposes a method to estimate the harmonic network impedance in HV networks as basis for calculating emission limits. It is a trade-off between the very simplified extrapolated impedance based on short-circuit power and a full system study for the determination of the worst-case impedance locus. It still requires a network model, but does not consider any possible switching states in the upstream network anymore. Based on the impedance scan of the simplified network and a reasonable margin introduced by a floating maximum based on a frequency width of 200 Hz, the harmonic impedance is calculated. The method is illustrated using three radial networks as example. The authors identify applicability to meshed networks as future scope.

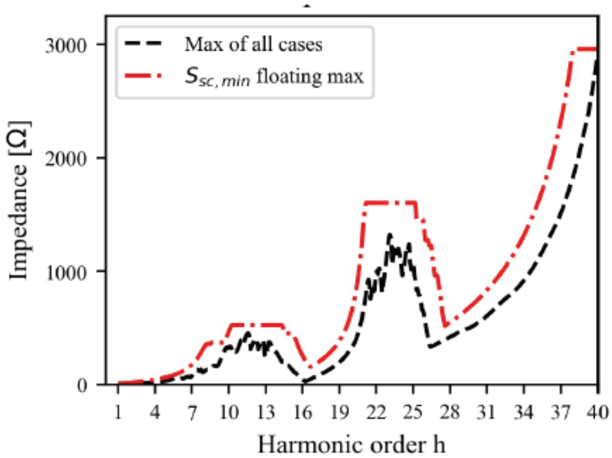

Fig. B3-2: Comparison of simplified method with the full analysis for Vores Elnet grid [B3-0440(DK)]

[B3-0135(SE)] applies the transfer function method as tool to evaluate the harmonic emission of a wind park. In particular, the method is used to analyse the interaction between different turbines as well as between turbines and the grid. For this purpose four different combinations of considering MV cables and LV customers have been considered (I: no cables/no LV cust.; II: no cables/LV cust. of single feeder; III: with cables/LV cust. of single feeder; IV: with cables/LV cust. of whole MV network). A three-turbine wind park of 2 MW is used for illustrating the application of the methodology. MV cables and other LV customers do not significantly affect interaction between turbines. In addition, they have no significant impact on the voltage distortion at turbine terminals for frequencies below the first resonance. However, at higher frequencies they can affect the overall transfer impedance characteristic significantly in terms of magnitudes and resonances.

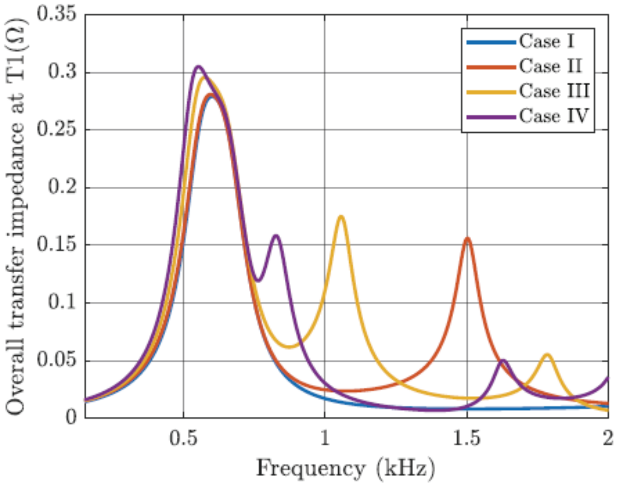

Fig. B3-3: Overall transfer impedance at wind park terminal for four cases [B3-0135(SE)]

[B3-0152(SE)] presents a stochastic aggregate representation of downstream LV networks to study harmonic impedance characteristic in MV networks taking uncertainties due to varying impedance characteristics of downstream networks into account. The methodology is applied to two Swedish MV networks to study the frequency-dependent impedance characteristic in the MV network. The results show that in the MV networks the first resonance appears at rather low frequencies (in one of the networks even below 50 Hz) and the variance of magnitude can vary in large ranges, while at frequencies higher than the first resonance the variation is much smaller. The authors emphasize that customer impedance model itself is a particular uncertainty, which requires further attention.

[B3-0462(DE)] studies the network harmonic impedance and the aggregated customer-side equivalent impedance at the LV busbar in LV networks depending on different realistic combinations of common household appliances. Three different scenarios in terms of time of the day (I: low demand, II: average demand, III: high demand) and in terms of evolution stage (A: past, B: present, C: future) are distinguished considering both an urban and a rural LV network. The results confirm that the particular customer configuration has a significant impact on the network harmonic impedance in LV networks. Furthermore, the increasing share of modern power electronic equipment increases the probability of resonance with a tendency to lower frequency of first resonance.

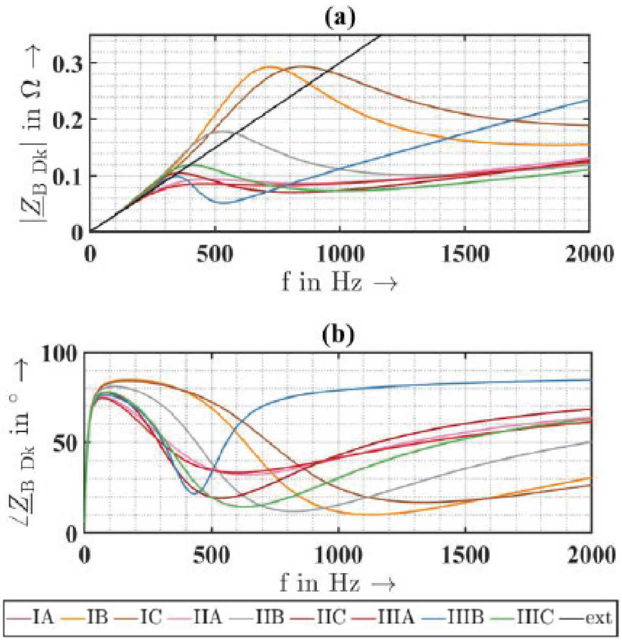

Fig. B3-4: Impedance characteristics of a urban LV network at LV busbar (a): Magnitude, (b): Phase angle [B3-0462(DE)]

[B3-0248(JP)] develops a methodology to include grid-connected inverters in frequency domain simulations for harmonic studies. The inverter is split into the filter part and control part, which both will influence the harmonic impedance and consequently the propagation of harmonics. While the filter-part can directly be added to the system admittance matrix, respective formulations are provided on how the control is included. The proposed methodology is finally applied to study the impedance characteristics in a one-inverter and a two-inverters scenario as well as the disturbance levels resulting from the emission spectrum of an additionally connected 6-pulse-rectifier. As expected, the impedance characteristics differs significantly between the scenarios and due to the introduction of additional resonances, an amplification of harmonics is observed compared to the reference scenario without inverters.

[B3-0566(DE)] is also focused on modelling of individual devices, but from the perspective of including the model in real-time simulations (hardware-in-the-loop systems). The presented method is based on the identification of the coupled Norton equivalent (CNE) and follows a Black Box approach. This has the advantage that the method can be applied to any equipment without detailed knowledge about circuits and control. The harmonic current response of the model is updated in real time depending on the applied supply voltage. This is only possible for (Black-Box) frequency domain models, as (White-Box) time domain models would require too long simulation times. The method is validated in a lab environment consisting of a programmable amplifier as source, a network impedance and a hardware-in-the-loop simulator simulating a radial fan as device under test.

Supraharmonics (2 kHz – 500 kHz)

This sub-block includes seven papers dealing with different aspects in the frequency range from 2 kHz mainly to 150 kHz, but also up to 500 kHz. The frequency range between 150 kHz and 500 kHz includes the FCC band, which attracts increasing attention to be used for power line communication (PLC) applications. While three papers are focused on modelling aspects in LV networks, three papers study the particular interaction between converters and grid as wells as between converters. This is complemented by one paper analysing the propagation of supraharmonics in MV networks.

[B3-0101(BE)] introduces a methodology for efficient (analytical) modelling of supraharmonic propagation in LV networks. It represents each element of the network by three chain matrices representing positive-, negative- and zero-sequence. Modell implementation for LV cable, MV/LV transformer and upstream MV grid as well as for single- and three-phase disturbance sources are explained in detail. The analytical (equation-based) implementation is much faster than any time domain simulation based on White-Box models. The application of the proposed methodology is illustrated by an example where a disturbance source (three-phase and single-phase) is connected at the end of a long cable. The results show that both damping and amplification of emission is possible in upstream propagation and that a significant difference exists between three-phase and single-phase sources.

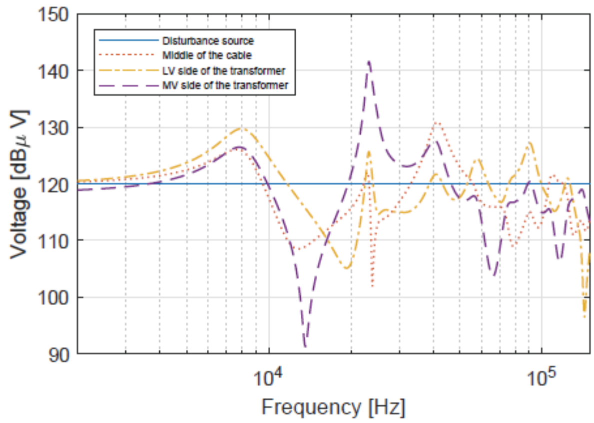

Fig. B3-5: Propagation on phase A of a 120 dBμV single-phase disturbance [B3-0101(BE)]

[B3-0469(FR)] presents a new, simplified method to obtain the transfer function in the frequency range from 9 kHz to 500 kHz between any two nodes in a network using the voltage ratios between the nodes. The comparison with two other approaches (circuit-based and ABCD-matrix-based) for a single cable shows a good match between simulations and measurements. The new method provides a simple way, e.g. to characterize the transmission channel for PLC communication applications, which is important in case of solving transmission issues.

[B3-0343(BE)] focuses specifically on the modelling of LV multi-conductor cables in the frequency range 2 kHz to 500 kHz. Three different techniques, namely four-terminal sensing, time-domain reflectometry and impedance measurements are used to identify the parameters of a four-conductor transmission line. The authors show, how the techniques complement each other in determining the model parameter values, which can simplify the transmission line model identification considerably. The methodology is demonstrated for two different types of cables and two different lengths. The results match well with the expectations.

[B3-0073(SE)] presents the study of supraharmonic currents in an installation consisting of two emission sources, namely multiple LED lamps (42-52 kHz) and a PV inverter (16 kHz), as well as different neighbouring devices (e.g. heat pump, water cooker) without supraharmonic emission. The neighbouring devices as well as the MV/LV transformer are connected via cables, for which the lengths were variated. Measurements have been carried out over longer time intervals in order to study the impact of different grid conditions to the supraharmonic currents. The results confirm that impedance configuration significantly determines the propagation characteristic. In presence of a weaker grid, less supraharmonic current flows to the network. The supraharmonic current to neighbouring devices also tends to decrease if the electrical distance between them increases.

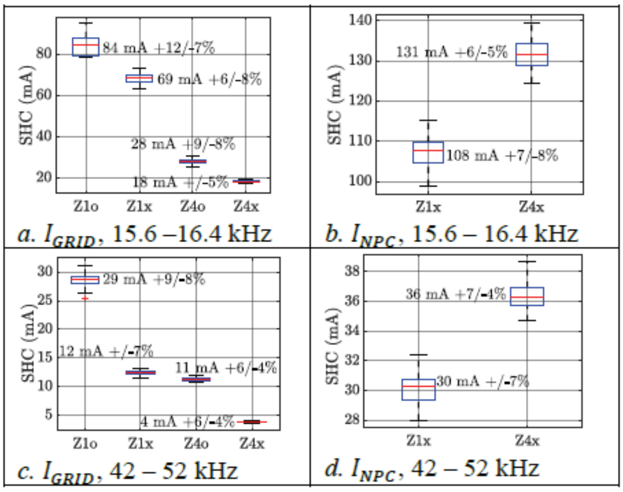

Fig. B3-6: Characterization of SH variations (x/o: neighbouring devices on/off; Z1/Z4: cable to supply transformer shortest/longest)

[B3-0112(SE)] studies the interaction of multiple converters focused on both AC and DC data centre applications with main focus on the beating effect, which is caused by slight difference between the switching frequencies of multiple converters. The paper simulates a "two source" environment with switching frequencies being 20 kHz and 20.01 kHz. Beating is clearly observed both in DC and AC application. One major outcome of the simulations is that the electrical distance between the two sources has a significant impact on the beating amplitude, which decreases exponentially with increasing length of cable between the converters, but converges to a constant value.

[B3-0723(JP)] models the impact of grid-connected inverters on the voltage disturbance levels in the MV network considering the frequency range 3 - 10 kHz. In case the switching frequency is close to the series resonance frequency of the system (about 6.2 kHz in the example), a significant amplification of voltages is observed. In a two-inverter configuration, the authors observe also the beating effect as studied in the previous paper. As the simulations have been performed without any further loads connected, the amplification is expected to be lower in real-world scenarios. The voltage magnitude at the emission frequency is not doubling from one-inverter to two-inverter scenario, which results from the different impedance conditions seen by one inverter between the two scenarios. This also confirms the findings of other papers that particular in the frequency range 2-150 kHz impedance configuration has a significant impact on the propagation of emission, even in the MV network.

[B3-0023(SE)] studies the propagation of supraharmonics in MV networks. Driving point impedances at different nodes and transfer impedances between nodes are analysed based on the detailed implementation of an existing 11 kV distribution network with eight feeders in MATLAB/Simulink. LV networks are included by a series circuit of models for the MV/LV distribution transformer and a lumped model of the LV customers. The impedance characteristic shows many narrow peaks in the supraharmonic range and differs significantly between feeders. Skin effect of MV lines has a significant impact on the magnitude of these resonance peaks. The impact of LV customers on the MV network is limited to the lower frequency range of up to 5 kHz. Finally the number of MV feeders itself has a significant impact on number of resonances and impedance magnitudes.

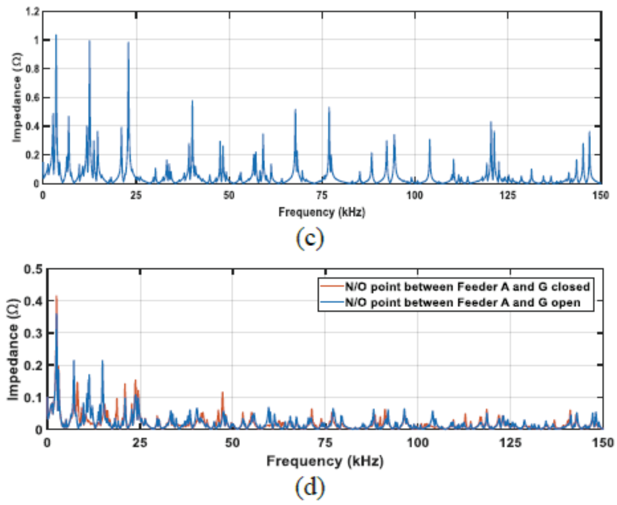

Fig. B3-7: MV Test Network Frequency Scan at Node 101 with (c): Feeder A, B, C and D and (d): Feeder A, B, C, D, E, F, G and H connected [B3-0023(SE)]

Other power quality phenomena

Only three papers study power quality phenomena other than distortion. While one paper deals with flicker, two papers study voltage dips, one paper from system perspective and one paper from customer/load perspective.

[B3-0290(AT)] uses a realistic large-scale MV distribution network model and develops respective flicker emission models of upstream HV network and connected customers in order to simulate the flicker levels in the MV network. The authors introduce different customer groups (e.g. household, agriculture, photovoltaics) and quantify their flicker emission by a flicker emission coefficient. A probabilistic simulation is performed to obtain the time characteristic of flicker levels at particular nodes in the MV network for a month. Simulations and measurements show a good match, proving that large-scale simulation of flicker levels is possible. The authors note that the parametrization of emission sources is still improvable.

[B3-0232(CN)] introduces a new index to evaluate the sag severity in a system individual for different regions. Therefore, all sag events of the system are divided into different clusters in terms of duration. For each cluster, the median of residual voltage is calculated. The region-specific index is obtained by calculating the average of all distances of sags in the considered region being lower than the respective (system) median line. The index aims to help utilities to evaluate the sag severity not only for a whole system, but also individually for different regions in the system, which might have different requirements in terms of sag performance. The application is demonstrated by using about one year sag data from a large Chinese city divided into 10 regions.

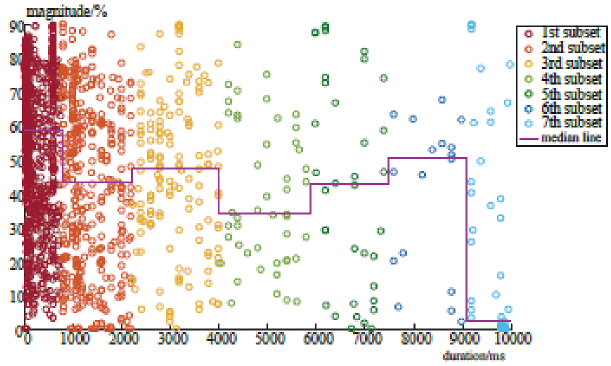

Fig. B3-8: Schematic diagram of duration cluster analysis results and respective median line [B3-0232(CN)]

[B3-0961(US)] highlights the fact that not every voltage sag will affect customer operation. Consequently, it is important to distinguish between disruptive and nuisance events in terms of more focused/prioritized filtering and reporting of alarms. The authors propose to analyse the time characteristic of RMS voltage together with the time characteristic of active power, both calculated cycle by cycle and updated each half cycle. In case a load loss is detected, the event is identified as possibly disruptive. This way an automatic classification of sags is possible with regard to its impact on customers and manual tagging is not required anymore. Results can easily be visualized by colours in the voltage magnitude vs. duration plot.

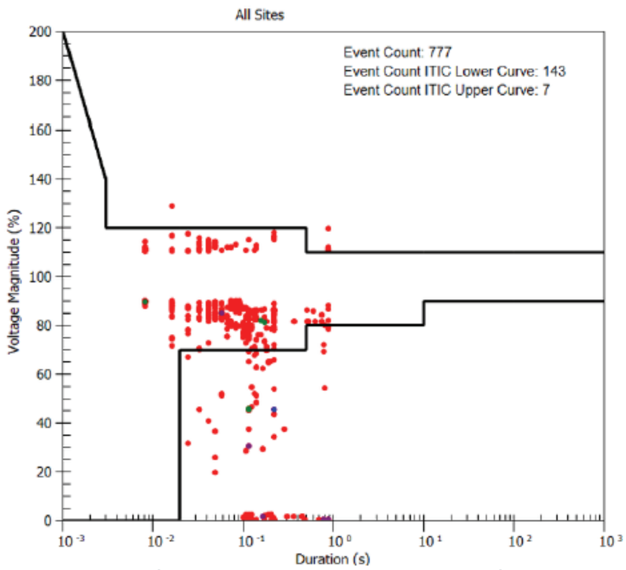

Fig. B3-9: RMS Variation Magnitude-Duration Scatter Plot Displaying Voltage Dips with Load Loss [B3-0961(US)]

Mitigation

This sub-block contains five papers. Besides a mitigation case study for flicker, the suitability of passive filters for harmonic mitigation is discussed. Three papers deal with improved control techniques for FACTS devices.

[B3-0287(EG)] analyses the flicker levels generated by a stainless steel factory with an electric arc furnace of 72 MW, which is connected via two lines from a 69 kV substation. Even with mitigation equipment installed at the steel plant, customers connected to the supplying substation suffered from flicker interferences. The authors carried out measurements in order to evaluate the flicker propagation and to recommend suitable additional mitigation. It has been found that the grid code requirements are significantly exceeded with long-term flicker severity being about 1.0 at the substation in two- and single-line operation (limit: 0.6). At the connection point of the steel factory, long-term flicker severity levels amount 3.1 and 4.2 respectively. The utility finally decided to accept the violations at the connection point of the factory, but separated all other customers.

The authors of [B3-1037(BR)] study the feasibility of passive harmonic filters under the aspect of the increased cost reduction of active filters using an industrial pulp and paper plant as example. A simulation has been developed to study the efficiency of the designed passive filter. Together with Dy transformers to connect to the MV system, the distortion in the industrial plant can be reduced significantly with just one filter tuned to the 11th harmonic from THD values in the voltage of up to 9.7 % to values not exceeding 0.9 %. In any case the authors emphasizes that detailed simulations shall always accompany the filter design.

In [B3-0309(EG)] a decoupled stationary reference frame PLL (phase locked loop) is proposed to make the sag/swell detection in a dynamic voltage restorer (DVR) more robust in presence of unbalances in the supply voltage. The theoretical background is provided and the difference to the simpler PLL without separate (decoupled) evaluation of positive and negative sequence is described. Time-domain simulations show that the simpler PLL under unbalanced voltage conditions results in a constant fluctuating error in the fundamental frequency estimation, which does not appear for the proposed decoupled PLL.

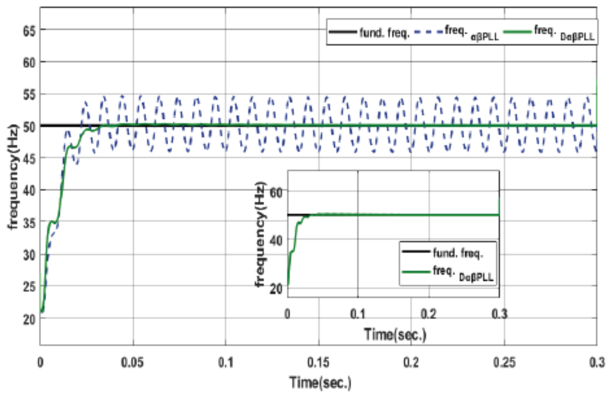

Fig. B3-10: Fundamental frequency estimation in unbalanced voltage conditions [B3-0309(EG)]

[B3-0422(EG)] proposes an enhanced and more robust control scheme for a static var compensator (SVC) as used in wind energy conversion systems. A more sophisticated model reference adaptive PI controller (MRAPI) replaces the traditionally used PI controller. Controller parameters are obtained by applying a Teacher learning based optimization algorithm. A simulation-based case study of a 22 kV wind park with three turbines shows the better performance of the new controller for sudden change in wind speed and load.
[B3-0139(EG)] deals with the improvement of the traditional used PI controller for a unified power flow controller (UPFC), which is used for improving power flow and voltage levels in a network. The authors introduce a fuzzy logic controller (FLC), whose parameters are optimized using harmony search algorithm. The improved performance is demonstrated using a Simulink implementation of the IEEE 15 bus system including a 1-MVA-UPFC. The presented results suggest that a further slight improvement is achieved with the proposed controller in terms of voltage profile, power flow and losses in the test system.

Measurement aspects

This sub-block contains five papers, where one paper deals with measurement accuracy of power quality instruments. Four papers study the frequency dependent transfer characteristics of MV voltage transformers and discuss different invasive and non-invasive methods for its identification.

[B3-0945(DE)] provides in its first part a detailed description of a software package, developed by the authors, to perform harmonic load flow simulations. A comparison between the developed package and two commercial network calculation packages is provided. Significant differences have been observed in the results of one commercial package. In the second part, the authors investigate the impact of different parameters of a measurement instrument, like resolution of A/D-converter or sampling rate on the accuracy of harmonic measurements using the respective IEC standard implementation by a Monte-Carlo-simulation. The choice of the window function for the Fourier transform has been found to have the most significant impact.

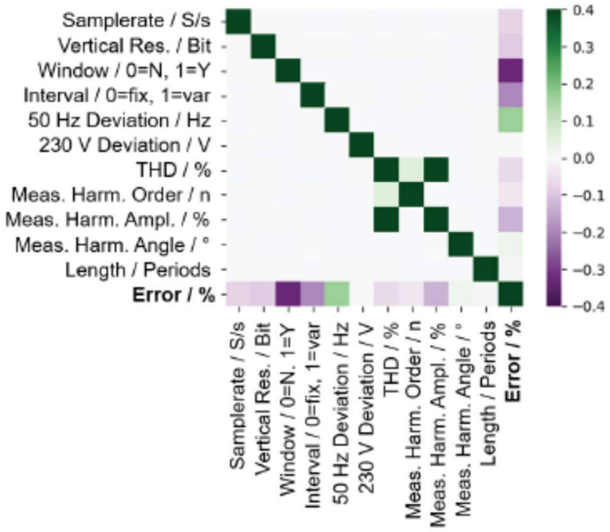

Fig. B3-11: Result of the correlation analysis for a PQI with variation of the whole state space for all parameters [B3-0945(DE)]

[B3-0765(IT)] introduces the European project IT4PQ, which runs in the framework of EMPIR (European Metrology Programme for Innovation and Research). One of the objectives is the study of the behaviour of the frequency response of voltage instrument transformers (VT) and current instrument transformers (CT) for MV application in order to support the activities in IEC TC38 to include respective requirements in future standards. Power quality parameters that can be influenced by instrument transformers are summarized and reference setups for the laboratory measurements are described. External influence parameters on the frequency response are identified and it has been shown that electric fields can have a significant impact on the measurement accuracy of low power voltage instrument transformers.

[B3-0369(GB)] studies the frequency response of five MV VTs in the laboratory under different secondary burden conditions. It has been found that in the considered frequency range up to 5 kHz significant resonances can exist, which cause ratio errors of up to 80 % and phase angle shifts up to 85° at certain frequencies. The authors emphasize that for characterizing a VT for possible calibration of harmonic measurements, it is essential to reproduce the in-situ burden at the final location as best as possible.

The authors of [B3-0230(AT)] use a standard testing device for Sweep Frequency Response Analysis (SFRA) to determine the frequency response of MV and HV VTs. The device has been modified in terms of its input impedance in order to achieve a good comparability with reference measurements. The main advantage of the device is its small size and weight, which enables frequency response measurements almost anywhere in the field. The device has been used to measure the frequency response of 47 MV and HV VTs. The results for the MV VTs are shown in Fig. B3-12 in terms of the relative application bandwidth for different acceptable ratio errors. The application bandwidth defines the maximum frequency up to which a harmonic voltage can be measured with a ratio error less than or equal to the specified one.

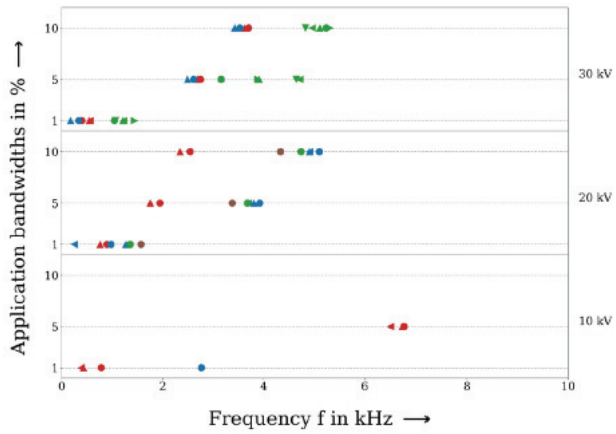

Fig. B3-12: Application bandwidth of medium voltage VTs determined with 1 MΩ SFRA [B3-0230(AT)]

While the measurement methods described in the former papers required the individual VT with primary and secondary side not connected in order to apply a generated frequency sweep, the authors of [B3-0216(DE)] developed an in-situ applicable method to identify the frequency response of MV VTs solely by connecting a standard PQ instrument with switchable burden. Ambient temperature can significantly impact the frequency response characteristic of a MV VT (e.g. it can shift the resonance by several hundreds of Hz) and has to be taken into account in case of a calibration. Therefore the authors propose a continuous monitoring technique, which in a first stage identifies the temperature-dependent frequency response of the VT in order to train an artificial neural network. This is implemented into a power quality instrument and enables a reliable real-time compensation of MV VT ratio errors.

Potential scope of discussion

Similar to the conference two years ago the accurate determination of frequency-dependent impedance remains a big challenge both for the frequency range below 2 kHz (harmonics) but especially for the frequency range above 2 kHz (supraharmonics). The accurate representation of customers at LV level covering the large diversity of appliances as well as the largely varying usage behaviour requires probabilistic modelling approaches, which still need significant further research.

The increasing importance of the frequency range above 2 kHz is also reflected in a significantly increased number of papers compared to the conference two years ago. While some reliable knowledge exists for the LV network up to 150 kHz, the need for studying the propagation towards the MV network as well as the extension to 500 kHz including the FCC band has started just now.

Nowadays, harmonic emission limits for larger customer installations are usually calculated by assuming balanced conditions. Recent research has shown that such assumptions do not hold true and particularly in LV networks triplen harmonics do not exclusively form zero-sequence systems. How these new findings affect the derivation of emission limits in the planning stage as well as the measurement-based determination of the customer emission in the operation stage has to be intensively discussed.

Another important aspect in power quality evaluation is the need for critical review, if established indices properly reflect existing and newly upcoming interference mechanisms. Furthermore, the link between disturbance levels and real impact on customer equipment and how to identify it, must gain higher importance in the future.

In terms of measuring power quality, in particular distortion, the accuracy of the whole measurement chain, which in most cases also includes external sensors has to be taken into account. Especially “traditional” instrument transformers have been designed for high accuracy at power frequency only and can exhibit high measurement errors for harmonics or supraharmonics. Beside the application bandwidth, which is commonly used to describe their suitability for distortion measurements, calibration procedures that take the continuously changing impact of external factors (e.g. temperature) into account need further attention in the future.

Table 3: Overview of papers in Block 3

Paper (No. and Title)		MS	RIF	PS
23	Propagation of supraharmonics in a medium-voltage network			I
73	Assessment of grid impedance impact on supraharmonic propagation	X		X
101	Efficient method to study the propagation of supraharmonics on the LV grid through symmetrical components and chain matrices			I
112	High frequency interaction of power electronics converters in AC and DC powered data centers			I
135	Application of transfer function method in a wind park for harmonic study			X
137	Comparing harmonic unbalance at multiple locations to characterize the unbalance			I
139	Improving power quality for distribution system using hybrid control technique			I
152	Application of a stochastic aggregate load model to study harmonic propagation in distribution networks			I
216	Methods for on-site qualification and calibration of inductive instrument voltage transformers for harmonic measurements		X	
230	Frequency response analysis to assess the application bandwidth of inductive voltage transformers		X	X
232	Evaluation method voltage sag severity from grid side based on point-to-line distance index			X
248	Extension of harmonic calculation considering grid-connected inverter			I
287	A case study for voltage flicker mitigation in large steel industry			X
290	Modelling of flicker in large real medium voltage distribution networks	X		
309	Voltage sag/swell detection based on decoupled stationary reference frame PLL in DVR			X
343	Distributed properties of multi-conductor low voltage cables at 2-500 kHz: Network analysis by four-terminal sensing, time-domain reflectometry and impedance measurements	X		X
351	Statistical analysis of field measurement data of harmonic currents in residential distribution systems			I
369	Voltage transformer harmonic characteristics for distribution power quality monitoring		X	
422	Adaptive control strategy of SVC in a wind energy conversion system (WECS) using advanced evolutionary algorithms			X
440	Novel intermediate method of impedance calculation for connection requirements to high voltage grids	X		
462	Impact of modern power electronic household equipment on harmonic resonance in public LV networks	X		
469	Computation of Transfer Functions using a bottom-up modelling approach in the 9 to 500 kHz frequency range			I
566	Dynamic implementation of harmonic behaviour for power hardware-in-the-loop real-time simulations			X
723	An experimental consideration of high-order harmonic resonance phenomenon caused by grid-connected inverter in parallel operation			I
748	Real case interaction between a sympathetic inrush and a resonant system	X		X
765	Assessment of instrument transformer accuracy for power quality measurements in distribution grids: recent activities and first results from the 19NRM05 IT4PQ project		X	
945	General framework for simulating power quality data processing			I
961	Automatically evaluating the impact to loads caused by voltage dips in electrical systems			I
1037	Passive filters are still a good solution for harmonics distortion mitigation			X

I: interactive poster presentation

Block 4: "Standardization, system monitoring, handling big data and regulatory issues"

Power quality standardization has to keep up with trends in distribution systems. Trends like the use of non-linear household appliances and the integration of non-linear renewable generation and charging units have been building up over the past years and need to be thoroughly analysed and understood. The aggregation of PQ phenomena of a large number of new appliances and interaction with already existing appliances connected to the distribution grid lead to a complex situation. In some cases, it will be important to respond appropriately before a tripping point is reached. Large-scale monitoring systems or campaigns are important in order to know the situation in the distribution grid and to recognize trends early. Applying machine learning and visualisation techniques is needed to analyse large amounts of data and to discern changes. Standardisation has to keep up and be amended in a timely manner.

New developments in standardization

New developments in standardization have the goal to maintain and enable efficient operation of the electric grid with adherence to the required quality. For this year's conference we received ten papers dealing with new developments in this field.

[B4-0065(DE)] presents the results of a D-A-CH-CZ survey on MV grid characteristics for the improvement of emission limit-allocation for large customer installations. Regarding power quality, the grid is optimally utilised if the disturbance levels meet but not exceed the compatibility levels in the low voltage grid. The actual harmonic and unbalance levels in medium and low voltage grids are often lower than the planning or compatibility levels. A maximum hosting capacity is introduced to ensure that the global contribution is not exceeded. This capacity corresponds to the power of all expected customer installations in the grid including also future connections. The maximum hosting capacity presently assumes that all customer installations are directly connected to the MV grid. The aim of this paper is to verify the assumptions behind the equation to calculate emission limits. The authors performed a survey related to the characteristics of typical MV grids and the distribution of directly and indirectly connected customer installations. Fig. B4-1 shows the ratio between the maximum power of customer installations and the agreed power. Using existing equations, the emission limits differ by a factor of four, which means that in case only LV customers are connected to an MV grid the global contribution is utilized by about 25%. The results of the survey show, that in many cases the dominating share of customers is connected to the downstream LV grids. This suggests adapting the share of compatibility levels between LV and MV grids for the calculation of emission limits. However, the level of adaption has to take further factors, like the total hosting capacity utilization or the power utilization, into account.

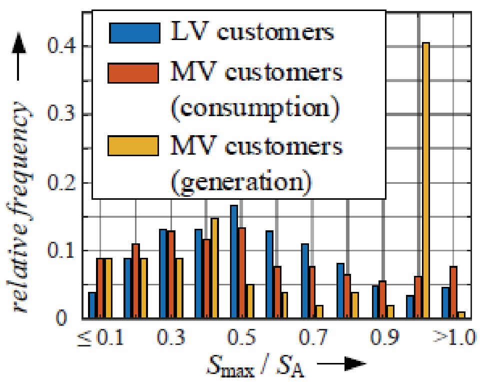

Fig. B4-1: Histogram of the ratio between maximum observed power and agreed power [B4-0065(DE)]

[B4-0274(CZ)] focuses on the proposed changes in the design of the current IEC flicker meter (FM) which are mainly related to the calculation of the flicker severity index P_{st}. The difference between a new flicker meter implementation and the existing one is identified through measurements in laboratory and field and through experiments. The field measurements were performed at different locations in public low voltage networks. The results are that the proposed FM tends to provide smaller P_{st} values than the current one and the proposed metric is less affected by peaks and rapid changes. Experiments were conducted with people in order to evaluate, which of the two FMs can better predict the properties of human vision and flicker perception. Depending on the waveform and frequency modulations, the current or proposed FM, or neither of them, is more favourable. In some cases, no clear conclusion is possible and one experiment suggests that neither of the two FMs is able to predict the outcome correctly. As there are still uncertainties with some configurations of the measurements, the authors suggest further research. A round table discussion (RT 19) is organised to address the future of flicker.

The authors of [B4-0727(SE)] describe first steps towards a standardized hosting capacity method. This method can help assessing where and when network strengthening is needed. The hosting capacity is limited by phenomena like overvoltages, thermal overloads, incorrect protection operation, increase in unbalance, or excessive levels of voltage or current distortion. When multiple phenomena are considered, the hosting capacity is the lowest of the values found for the different phenomena. A standardised hosting capacity must fulfil consensus, stability, transparency, harmonisation, and interoperability requirements. Moreover, standardization enables benchmarking across network operators, countries, regions, and design methods. For stochastic methods, some standard models for handling the different uncertainties are required and especially for non-typical situations, certain approaches to aggregation, parameter selection and handling of distribution of uncertainties need to be modified.

In [B4-0772(DE)], new guidelines to determine the harmonic emission of an operating customer installation based on field measurements are proposed. The proposed framework consists of two stages, the first one analysing the current harmonics, while the second analyses the voltage harmonic contribution. Resulting from the framework are two flowcharts. In a first flow chart, the current emissions are assessed. If the currents are within a set limit, the installation complies with the emission limits. If they are well above the limits, the installation does not comply with the limits. If they surpass the limits slightly (up to factor 2), the voltage contribution assessment flowchart is used and if the limits are not surpassed, the installation is deemed to comply with the emission limits. Based on this procedure, several sites have been analysed. It showed that the assessment of harmonic currents alone could result in a number of cases in a non-compliance decision, which is not justified if the harmonic voltage contribution is evaluated. The proposed framework can therefore improve the reliability of the compliance assessment. For further analyses, due to the inherent variation of emissions, a continuous monitoring of harmonic emissions is suggested. Additionally, the need of additional input data, particularly the supply-side harmonic impedance, has been identified.

A new definition of interharmonic is presented in [B4-0841(CZ)]. The new subgroups are better able to tackle the main problem caused by interharmonics, the light flicker produced by modern lamp technologies, which cannot be assessed by the IEC flicker meter. Past implementations of subgroups are mostly subgroups based between two harmonics. As it has been determined in this paper however, the sensitivity to flicker around even harmonics is considerably lower than around odd harmonics. This means that subgroups should be centred around odd and even harmonics and therefore allow for more relaxed limits around even harmonics. In a numerical case study, the robustness of the new metric versus the desynchronization of the window used for the DFT with respect to the system fundamental frequency and versus the inaccuracy allowed by the requirements of the voltage measurement chain has been presented.

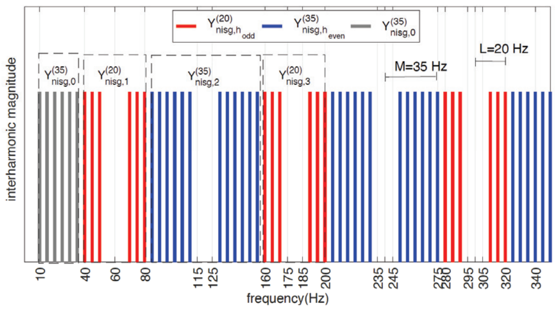

Fig. B4-2: New interharmonic subgroups corresponding to L=20 Hz and M=35 Hz [B4-0841(CZ)]

[B4-0852(US)] presents ongoing and recently finished power quality standards and technical reports by the working groups sponsored by the Power Quality subcommittee of the IEEE Power & Energy Society. In this paper, the seven working groups operating within the Subcommittee Power Quality of the IEEE PES T&S Committee are examined in detail and their ongoing as well as shortly finished projects are presented. The working groups are divided in the following directions: Working Groups on harmonics, voltage quality, monitoring electric power quality, power quality solutions, voltage imbalance, economic evaluation of voltage sags and on power quality data analysis.

Two different methods used in two different locations are compared to determine limits of the harmonic emissions from grid users. The methods discussed in [B4-0932(US)] include the limits prescribed by IEEE 519 used in the United States and the limits imposed by the IEC standard used in the D-A-CH-CZ region. As the IEC method has a more systematic approach in comparison to the approach of the IEEE method, the paper focuses on the necessary adaptations to the IEC method to factor for the differences in power grids between both regions. Comparing the results for the harmonic limits from both methods shows that the limits set by the adapted IEC method are tighter than those set by the IEEE method for the lower harmonic orders as well as the triplen odd harmonic orders. As for the higher harmonics, the IEEE method shows limits that are more restrictive. It is then concluded that the IEEE method lacks of a formal structure, which can result in potential voltage harmonic limit violations. The IEEE method also does not consider zero-sequence harmonics, which is especially important in the US power grid since it is mostly solidly grounded. The IEC derived method can be adapted for use in American power grids, which delivers less optimistic but more realistic limits, and the IEC method enables grid operators to optimize the utilization of the network's harmonic hosting capacity.

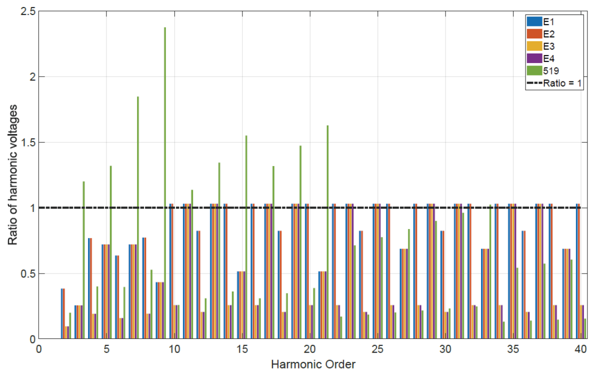

Fig. B4-3: Utilization of voltage harmonic limits for all 4 considered variants of IEC and for IEE519 [B4-0932(US)]

The third edition of the Austrian-Czech-Swiss-German technical rule described in [B4-1009(DE)] applies to customer installations connected to low, medium, and high voltage networks. It is a guideline for the calculation of emission limits, covering voltage changes, flicker, unbalance, harmonics, interharmonics, supraharmonics, commutation notches and mains signalling. Commonly used mitigation measures for these phenomena are described as well. Further, it describes the basic principles of allocation methods and the general assessment methodology. The equations to calculate emission limits and the individualized assessment procedures for each disturbance phenomenon are provided. The last part contains a set of examples that illustrate the application of the assessment procedures and emission limit calculations. Although there are many improvements in the third edition, there are still open issues like the topic of supraharmonics, the network-wide harmonic propagation or the sometimes-observed miscorrelation between the higher flicker levels and respective complaints that require a better understanding.

In [B4-1031(IR)], a new correction factor for IEC 60364-5-52 standard in cable calculations under harmonic conditions is presented. The effects of a high number of nonlinear loads connected to the distribution grid are analysed. The results show that a total harmonic distortion current of 57% and a total harmonic distortion voltage of 8.5% are appearing in this case. Not only are those values above the Iranian standard, but they also lead to higher neutral currents than phase currents. Given that normally the neutral current cross-sections are smaller than the phase current cross-sections, this poses a problem to the distribution grid. This means that in case of high harmonic distortion, there is the need for a correction factor to account for the increasing phase and neutral currents. Upon inspection of the IEC 60364-5-52 standard, it has been found, that the factor included in the IEC standard has a non-monotonic behaviour. The proposed adaptions to the IEC standard propose to determine a monotonic correction factor.

The authors of [B4-1150(CH)] describe the pre-normalization of grid impedance measurements in the power line communication frequency band. Power line frequency and time dependent grid impedance (FTdGI) influences the propagation of the power line communication (PLC) signals and influences the communication with smart meters. Currently, the precise measurement of the power line impedance is ill-defined and only possible with a few instruments. A large number of existing standards were compared with the results of measuring campaigns realised on sites in Europe. For all specified standard impedances, a higher value for the frequency dependent grid impedance (FDGI) was found compared to most of the cases when measuring the low voltage distribution grid in European locations. The defined standard reference impedance should be representative of average frequency behaviour of low voltage AC grid in Europe. Moreover, it should contain the dynamic range of impedance with stronger variations of phase and magnitude. Four grid impedance analysers with different characteristics were evaluated within the project. Two measurement modes, unenergized and energized 230 V / 50 Hz, were compared in the laboratories. All the results are compared with those obtained by METAS using an unenergized calibrated LCR meter. The correlation between the results with different equipment is good for the unenergized mode. For the energized mode, there are two ways of feeding the static reference impedance. It is possible to use an electric grid simulator or directly use the electric grid. The connection of the impedance analysers to the protective earth or to the neutral conductor and the use of a grid simulator can affect the measurement results significantly. Therefore, the measuring conditions are important to quantify the comparison. Fig. B4-4 shows the results of the energized measurements. For this purpose, the standard reference impedance defined in the Z-NET project is used. The results show that the magnitude at resonance differs only slightly from the unenergized measurements. A static impedance reference was specified based on available results. This reference can be used for the evaluation or the calibration of grid impedance analysers.

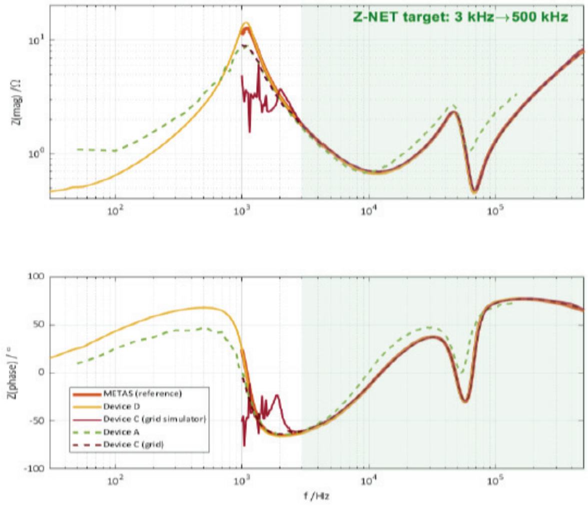

Fig. B4-4: Results of the comparative energized measurements of the Z-NET Static Impedance Reference [B4-1150(CH)]

Large scale PQ monitoring systems and campaigns

For this CIRED ten papers present findings related to large scale monitoring systems and campaigns, which have been built or undertaken in order to capture the different parameters of power quality in the respective distribution grid and to identify and understand trends and disturbances.

In [B4-0049(SE)], Short-Time Fourier Transform (STFT) is used to analyse the spectrum of real transients from a LV network. At first, several configurations for the STFT are tested and applied to different waveform lengths. Secondly, the transients from some random devices, an induction stove as well as from a PV panel have been analysed. It has been found that the transients from the random devices, the STFT has either a higher energy spectrum for frequencies below 3kHz or lower energy spectrum spread along the frequency domain. When analysing the transients originating from the induction stove, transients in the frequency range between 2.1 and 4.8 kHz with power frequencies over -20dB/Hz have been measured. In the case of the PV panel (Fig. B4-5), frequencies between 0.1 Hz and 0.2 Hz have more than double the power during the transient, while a second range from 1.375 kHz to 1.875 kHz sees power frequencies within -11.73 dB/Hz and -19.01 dB/Hz. A third range between 16.07 kHz and 16.52 kHz has power frequency values between -18 and -19 dB/Hz.

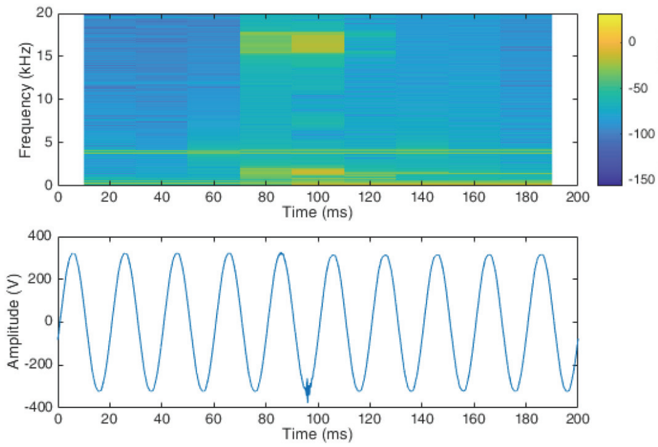

Fig. B4-5: STFT of oscillatory transients from the PV panel [B4-0049(SE)]

A new approach for estimating a safe hosting capacity in terms of harmonic distortion is proposed in [B4-0076(SE)]. This approach is based on standard limits for harmonic voltages and currents. Using the highest allowable currents for each harmonic with an impact factor k=0.1, while assuming no cancellation or aggregation, permits to establish a conservative and therefore lower bound on allowable harmonic devices at different positions in a grid. Using existing grid impedance values from almost 60'000 LV customers in Sweden, the safe hosting capacity for each harmonic has been determined. Fig. B4-6 shows the 5th percentile, 10th percentile, and the median. The lowest values were found for triple and even harmonics with a minimum for the 6th harmonic with a median value of 0.62, which then determines the total harmonic capacity for a LV customer. This being a very conservative method, using more realistic values of k=0.9 and an aggregation exponent of α=1.4, 6th harmonic values of factor 18 higher are found. This method therefore allows for a lower bound estimation of safe integration of new loads, the determination of critical harmonics for certain grids as well as adaptations for more realistic values for safe harmonic hosting capacities.

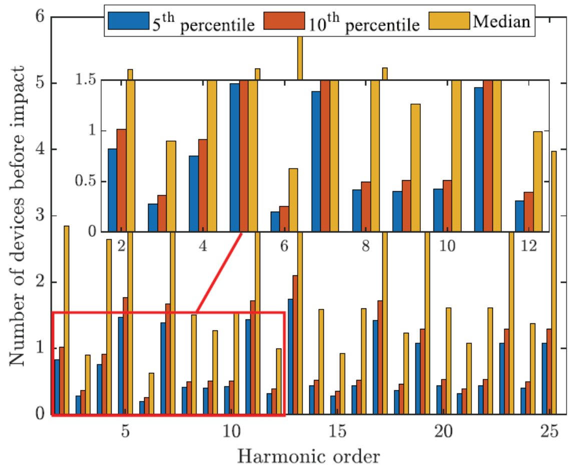

Fig. B4-6: Safe harmonic hosting capacity for 60'000 LV customers, presented in 5th percentile, 10th percentile and median [B4-0076(SE)]

Results of harmonic voltage measurements at multiple locations in a low voltage network are presented in [B4-0080(SE)]. In a first step, it is shown that the existing voltage levels from characteristic harmonics for the measured locations are well below the standard limits. In a second step, correlation matrices are calculated for different harmonics at the same location, different harmonics at different locations and correlation matrices for specific harmonics in different locations. This paper concludes that there is a strong correlation in low order harmonics up to the 13th order excluding triple order harmonics for the locations connected to the same LV network. The fact, that these low order harmonics can be found in several locations in the same grid, means that those harmonic levels originate at LV grid level or higher and that local loads only have limited impact on those harmonic levels. As an overview, Fig. B4-7 shows the correlations for locations in the same LV grid (1-5), as well as correlations to locations further away (6-9).

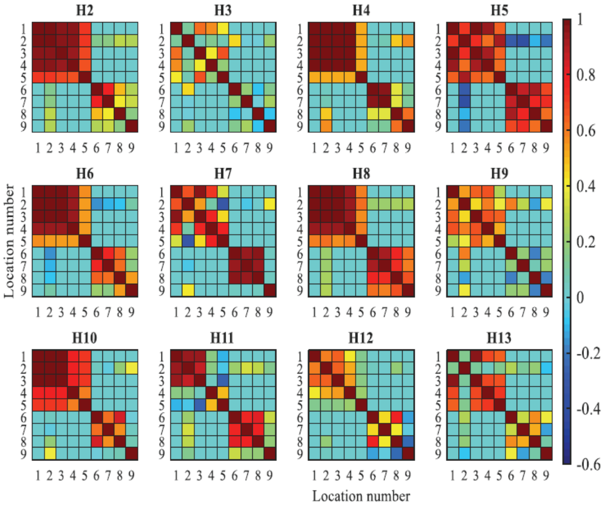

Fig. B4-7: Correlation coefficients for Harmonics 2 to 13 between all measured locations [B4-0080(SE)]

[B4-0370(GB)] analyses power quality data from 33kV distribution networks gathered during 2020. The network power quality will be affected through the growing number of low carbon technologies (LCT) like solar PV sites and electric vehicle charging points. Two areas with different penetrations of LCTs were chosen for the analysis. Power quality monitors were installed at every available substation within the analysed 33kV networks. The measurements show that the sites in the areas with a higher LCT penetration see a greater variation in multiple harmonic orders. Other PQ measures are short- and long-term flicker, voltage total harmonic distortion and voltage unbalance. Similar to the results for the voltage harmonics, the magnitudes of the other PQ measurements vary between the different areas and across the sites within an area. Measurements of the 16th voltage harmonic at four different sites in the area with high LCT penetration show, there can be substantial variations in aggregated PQ values in the long term. The results are shown in Fig.B4-8. Although the sites show similar trends in terms of when values rise and fall, the magnitudes are consistently higher at the solar PV sites. In addition, the range of variations for all voltage harmonic orders at sites that are solar PV farms is higher compared to sites without solar PV farms.

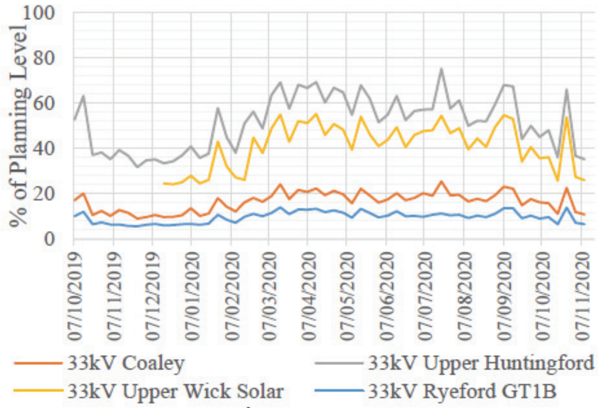

Fig. B4-8: Weekly 95th percentile aggregates of the 16th voltage harmonic at four sites with high LCT penetration [B4-0370(GB)]

Paper [B4-0372(GB)] deals with the development of an integrated platform for power quality monitoring. With an integrated PQ data collection and analysis platform, valuable resources for the manual analysis of PQ data are freed up and time is saved. There are several requirements for such a platform like vendor-agnostic, integration of several PQ analysis features, ease of use, integration with other systems and cybersecurity. The authors decided to use an already existing monitoring platform and then add the required PQ analysis features. The main features of the platform are the acquisition and processing of data from various PQ monitors, summarising PQ data and system status, visualising PQ data over time, browsing through events, viewing event recordings and producing PQ assessment and compliance reports. The developed platform features automated PQ data retrieval, processing, visualisation, notification and reporting as well as monitoring fleet management. However, the platform continues to be developed and new features like machine learning applications may be included.

In [B4-0438(DE)], the feasibility of selected measurement methods in the frequency range 2-150 kHz for long-term field measurements is studied. Measurements in public low voltage locations have been performed using two different methods namely the CISPR 16-1-1 method and the method specified in the standard IEC 61000-4-7. The disturbances measured are coming from a PV inverter and from EV chargers. Distinct disturbances form the PV inverter could be identified at 16 kHz and its second harmonic at 32 kHz. The EV chargers have disturbances at 10 kHz from the switching frequency of the on-board charger, as well as at 18 kHz and 36 kHz from the switching frequency of the fast charger and its second harmonic. In both cases, the highest disturbance levels during the measurement period are well below the compatibility levels. It has been shown that the QP_{max} values from the CISPR method exceed the values in the consecutive RMS aggregation of the IEC method. However, the CISPR method provides lower values than the IEC method for the 99th and 100th percentiles of the consecutive maximum values. This shows that while the CISPR method is suitable for the assessment against compatibility levels, it tends to overestimate the impact of disturbances on additional thermal stress and it tends to underestimate the possible malfunction rate of connected electronic equipment. On the other hand, the IEC method is reflective of interference mechanisms but has limited application for the assessment of disturbance levels against compatibility levels. However, using the IEC method, the 99th and 100th percentiles of the maximum aggregated values are reliable at giving conservative estimates of the QP_{max} values.

The automatic identification of correlations in large amounts of power quality data from long-term measurement campaigns is described in [B4-0576(DE)]. To analyse large amounts of data from PQ monitoring in an efficient way, automatic data mining methods are required. In this paper, an automatic algorithm for identifying correlations in the trend between different PQ parameters and measurement sites is introduced. Correlation can be used as a measure of similarity between multiple time series of PQ parameters. Shorter time intervals or a transformation combined with averaging can lead to better results. For the analysis, voltage and current measurements from 21 different sites with a duration of up to 3 years were taken. The PQ parameters monitored include voltage parameters like voltage RMS, voltage unbalance, total harmonic voltage distortion, harmonic voltages and current parameters like fundamental currents and harmonic currents. The long-term measurement analyses show that the most common correlation between PQ parameters is between total harmonic voltage distortion and the 5th harmonic voltage. Future research will cover the analysis of time varying correlations and the application of correlation analysis on time series itself.

The authors of [B4-0950(ES)] use PQ data mainly to assess compliance with limits. The measurements are taken from an open power quality database where measurements from two different PQ monitors show data from different sites around the world. In this paper, only harmonic voltage data from Europe are considered and especially higher odd harmonic orders and even harmonics. From the study of long, medium and short-term PQ characteristics, information about trends, seasonal effects or deviations from "typical" values can be obtained. Yearly emission of higher-order odd voltage harmonics for four different cities is analysed. The results are visualized as boxplots that show the various harmonic amplitudes (Fig. B4-9 (a)) or as 50, 95, and 99 percentiles over the year, which represent the values from higher-order odd voltage harmonics (Fig. B4-9 (b)). Seasonal variations of electricity usage or the connection/disconnection of devices during certain times are potential reasons for these variations. The plots show an weekly pattern in the behaviour how people use electricity and for most orders and sites, the magnitude is reduced during the weekend.

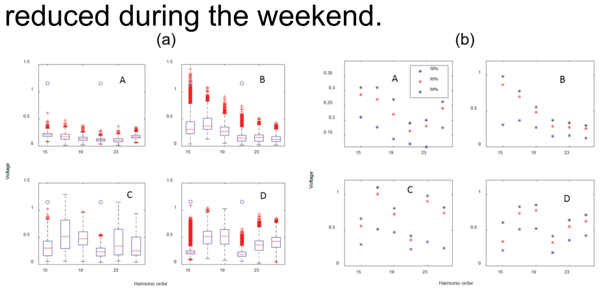

Fig. B4-9: (a): Boxplot of higher-order odd voltage harmonics at four sites, (b): 50, 95, 99 percentiles of higher-order odd voltage harmonics at four sites [B4-0950(ES)]

Paper [B4-1051(FL)] deals with power quality data management and data analysis. As available data from distribution networks are plenty and diverse, complex automated pre-processing, integration, and analyses are needed. Right now, international standards for PQ management practices and technical specifications of the monitoring systems are missing. The authors state that PQ management should be an integral part of distribution network design, operation and maintenance. Right now, the standard series IEC TS 63222 is being developed which defines use cases for PQ management and provides guidance for PQ monitoring systems. Open and common data formats, standardized communication protocols and flexible databases would all be beneficial for a better data management. Distribution management system (DMS) and supervisory control and data acquisition (SCADA) are two available systems for PQ data management in distribution networks, which have methods for data collection, transfer and storing and have some standards. The analysis method feasible in practice for PQ management in modern distribution networks remains to be determined. The analysis tools should be able to handle increasing quantities of data of various sources and types. Moreover, they should enable financial benefits of PQ management and consider the emerging PQ issues like interharmonics and voltage variations.

[B4-1132(DE)] describes site indices for high frequency harmonics for long term power quality monitoring. A common approach for reducing the data without losing its properties are site indices. Including the measurement of supraharmonics in the range from 2-150 kHz in long term monitoring systems drastically increases the amount of data. Consequently, new forms of data aggregation are necessary to retain information of the measurements in a highly compressed way. This paper presents a new approach for the aggregation of supraharmonics. The objective is to calculate indices, which are easy to interpret and visualize, and to compress the measurements. A first step to reduce the data size is by calculating and aggregating the measurements locally on the device and only sending the results to the monitoring server. For further aggregation, the lowest reserve of a specific parameter is used to represent the PQI of the site. In this study, the limits given in the IEC 61000-2-2 standard were utilized. With the resulting site indices, a straightforward visualization, interpretation, and comparison of the supraharmonics is possible and harmonics exceeding the prescribed limits are easily identifiable.

Visualization and machine learning for PQ big data

As monitoring and measurement systems are very sophisticated today, large amounts of data will easily be produced and have to be analysed in an efficient way. Manual analysis of all data will generally be no option. Consequently, machine learning and visualization of results using effective algorithms are of great interest. Five papers presenting different strategies have been submitted for this CIRED.

In [B4-0030(SE)], the visualisation of results from unsupervised deep learning is discussed. The generated graphs with daily, weekly and seasonal variations in harmonic voltages allow the interpretation of the results without having to understand the mathematical details of the method. The goal of the deep learning approach is the power system data analysis without pre-defined features and the extraction of the harmonic patterns. The presented method results in three plots. They show the two most dominant patterns, the patterns' spread and the results relevance. PQ data sets are from a continuous PQ measurement in a Northern Swedish distribution system. The PQ monitors are installed at MV (10 kV) and LV (0.4 kV). The measurement data consist of 10-min values for harmonics 2 through 50. The 3rd, 5th, 7th, and 9th harmonics are analysed in detail. In Table 4, the correlations between the patterns for each harmonic are listed. The low correlation of pattern spread for H3 points out, that it does not spread from one voltage level to another. For H5 and H7 it is different. Both show a high correlation between the patterns and between the voltage levels. It confirms that these harmonics have the same source and that they propagate through MV/LV transformers. The results show that inferences related to the daily variations, seasonality, origin, and propagation of harmonics could be obtained simply by the visualization of the DL results. The correlations between the patters were used to confirm the inferences given by the visualisation.

Table 4: Correlation between the patterns for each harmonic [B4-0030(SE)]

Correlation (%)	H3	H5	H7	H9
Pattern 1 and 2 in 0.4 kV	67	93	92	74
Pattern 1 and 2 in 10 kV	78	94	91	42
Pattern 1 in 0.4 kV and 10 kV	-51	97	93	-72
Pattern 2 in 0.4 kV and 10 kV	-67	98	96	-35
Spread in 0.4 kV and 10 kV	12	96	78	-68

[B4-0071(SE)] discusses graphical methods for presenting harmonic variations for different timescales and categorizes them in a systematic way. In addition, it discusses various methods for presenting harmonic variation and extracting knowledge from big data. The question is how to extract knowledge about harmonics' behaviour in an efficient way. Due to the time varying characteristics of current and voltage harmonics, the time scales of a few cycles up to a year cannot be neglected. The graphical display methods are classified based on the application of each method and the time scope. Harmonics can be expressed in time or frequency domain. For the aggregation and investigation of harmonic impact on equipment, the time domain can be more useful. The presented graphical methods are a spectrogram, a space phasor model, daily patterns, a time-series colour-plot, a correlation matrix, box plots, histograms, polar plots, and machine learning tools to extract patterns.

The authors of [B4-0160(SE)] provide a graphical tool to handle two different data inputs, namely individual interharmonics components in time-series and broadband spectra. Spectrograms allow an easy interpretation of interharmonics as they show the evolution of a spectrum with time. However, the graphical analysis is only suitable for a short period. For a long-term measurement, the use of an automatic tool is required. For a beneficial application, the method should be able to accurately estimate the frequency and the magnitude of the interharmonics or get characteristics of the broadband spectrum if such is present. This paper focuses on the application of deep learning to find patterns of interharmonics. The output of the DL method for time-series are main patterns of variations in PQ data. In this study, the DL method was applied to measurements of the aggregated values of the interharmonic currents between 50 Hz and 100 Hz over one year. Fig.B4-10 (a) shows the results provided by the DL method for interharmonics' currents. The distribution of the three clusters over one year is shown in Fig.B4-10 (b). The colours represent how the daily distortion was classified. The lowest distortion days and duration of interharmonic currents (pattern 3) are predominant in winter. To get the data for spectrograms, one sample of 10-second duration was extracted every 10 minutes for 24 hours. This leads to 144 spectrograms per day. Fig. B4-11 shows the cluster distribution over one day as well as the solar elevation angle. Cluster 1 appears mostly around sunrise and sunset but sometimes in the middle of the day. Cluster 2 does not present interharmonic components and appears when there is no sunlight. Cluster 3 presents mixed frequency components and appears during the PV production. The results of this study show that DL methods can be used in time-series measurements to find daily-patterns for individual interharmonics. Moreover, the method provides a solution to handle patterns of interharmonics in a range of frequency instead of an individual component.

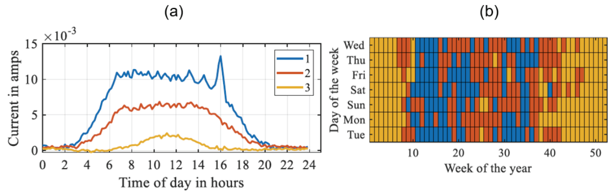

Fig. B4-10: Deep learning results for interharmonics between 50 and 100 Hz: (a) reconstructed patterns, (b) patterns spread over one year [B4-0160(SE)]

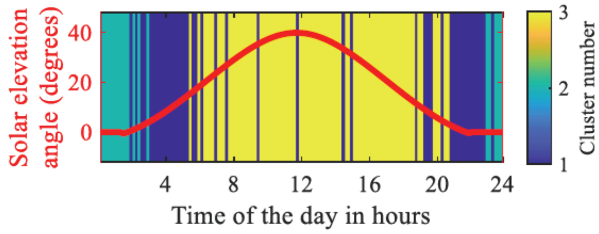

Fig. B4-11: DL results with patterns distribution and solar elevation angle for a specific day [B4-0160(SE)]

[B4-0575(FR)] deals with the harmonic risk estimation for LV networks by machine learning. Enedis, the main French distribution system operator (DSO), aims at obtaining a mapping of the harmonic risks for all its LV networks that considers various power electronics development scenarios in order to assess their impact. Such estimation is complex, as it requires extensive disturbance modelling for various grid situations. Thus, the authors decided to use machine-learning techniques for a more efficient computation. The output quantities provided by the model must be an image of the harmonic risk of the estimated networks. The considered output quantity is the maximal total harmonic distortion KPI for each network. The same database and dataset were used to train the machine-learning model with five different algorithms. After a first evaluation of the initial training algorithms, several parameters were adjusted to optimize the algorithms. In a last step the tuned machine-learning model was integrated into the risk estimation tool The finished tool allows any

DSO to select one or more LV networks, configure some model input quantities and run a harmonic risk estimation. However, the first results need to be consolidated because the new power electronics equipment model that was used is only based on assumptions and does not take measurements or harmonic dispersion into account.

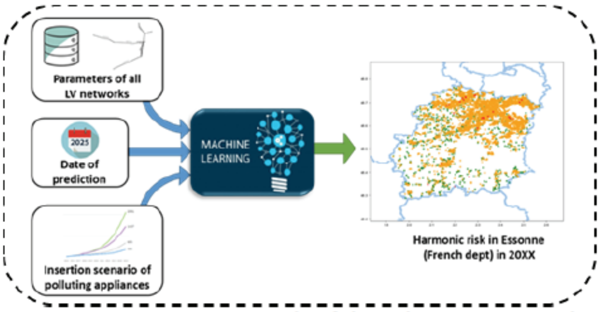

Fig. B4-12: Operating principle of the risk estimation tool [B4-0575(FR)]

In [B4-0871(FR)] machine-learning techniques are employed to predict the harmonic currents originating from most widespread power electronic devices and compared with time domain (TD) models. To achieve this goal, firstly a measurement-based time domain model needs to be built. It is determined by measuring the emitted harmonic currents following harmonic voltages as input, whose amplitudes and phases vary randomly. This model is then rebuilt in MATLAB Simulink to have a digital representation of the observed element. The influence of the network on the observed element is added to the model. As machine learning techniques, artificial neural network, support vector regression and decision tree regression machine learning models have been applied. Using a condensed set of measurements from input to the model in Simulink and its output is then used for the training of the three machine learning models. The output from the trained models show very similar current behaviour compared to the measured currents. The advantage of using machine learning models is that once the model is trained, it does not need additional tuning of the parameters whenever the supply conditions evolve, whereas the TD approach needs additional tuning and simulation when conditions change.

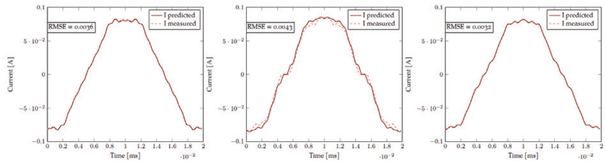

Fig. B4-13: LED harmonic current prediction using ML methods (a: ANN, b: SVR, c: DTR) [B4-0871(FR)]

PQ regulation, disturbances and customer issues

In this sub block, seven papers discuss the issues related to disturbances and customer issues as well as regulation. Three papers from Brazil examine the issue of regulation of damage claims and the view of distribution system operators and possible measures at customer sites.

The goal of the paper [B4-0085(EG)] is to mitigate inter-area oscillations due to different disturbances using a battery energy storage system (BESS) with a fuzzy-based control system. For this goal, a model with two different areas with a significant generation/load mismatch between both areas, coupled with a long transmission line, is used. In a first study, one of the two generators from one area increased its output by 0.05 p.u. for a duration of 0.2 s. When no BESS was used, this resulted in an oscillation in both active and reactive power transfer through the line, which increased cycle by cycle and consequently, the system became unstable. When BESS where used in both areas, the oscillations could be counteracted and the system remained stable. In a second study, the effect of switching one cable connecting both areas on the stability of the system was examined. In this case, around 3 s after the disconnection of the cable, the system loses its synchronicity (Fig. B4-14). As in the first study, employing a BESS in both areas could alleviate the loss of synchronicity by injecting power following the fuzzy logic control. As a conclusion, it seems that BESS systems have a great importance in reducing the adverse impacts of inter-area power oscillations on the transmitted power quality and lowering the blackout vulnerability.

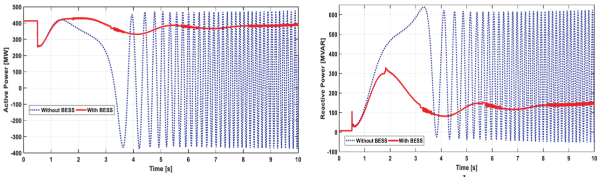

a b

Fig. B4-14: Inter area power flows due to disconnection of interconnecting tie-line for a) active and b) reactive power [B4-0085(EG)]

[B4-0090(SE)] analyses the risk of server outages. As server equipment is supplied by DC current from power supplies, they are sensitive to voltage dips in the AC system as that translates in dips in the DC system as well. Therefore, voltage dips caused by faults in the internal power supply system of the data centre are analysed. As benchmark for possible outage, the voltage-tolerance guideline of the Information Technology Industry Council has been used. A server layout with an internal power supply system (IPSS) has been modelled as subject of the analysis. A 10m single-phase cable connected to the load bus is determined to be the most sensible section of the IPSS. Depending on the location of the fault in the cable, the voltage drop might be large enough to affect the neighbouring buses and provoke further server equipment to be lost. Depending on the cable length of one server cluster to the uninterrupted power supply unit, the critical fault length in the 10m cable is longer or shorter and therefore the risk of affecting neighbouring server racks can be higher or lower. When including the failure rates of the cable in question, the failure rate of parts of the server cluster can be calculated for several layouts. It has been determined that in the studied system, a maximum of 33.33% of the servers could fail due to a fault in one of the 10m cables.

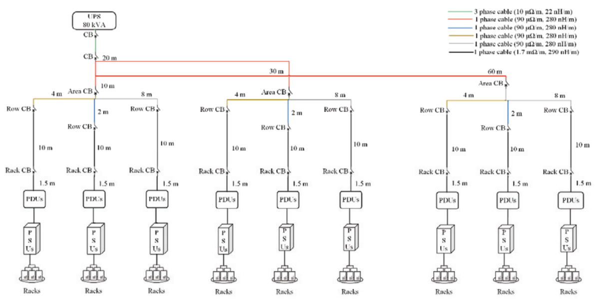

Fig. B4-15: The studied IPSS structure of the data centre [B4-0090(SE)]

The Brazilian regulations assign damage compensations of consumer appliances to the power companies. Therefore, the power companies have sought to assess possible impacts of events that occurred in the power grid and the resulting voltage disturbances. In the paper [B4-0191(BR)], the different types of occurrences in the Brazilian supply grid that cause disturbances in voltage were analysed. Types of disturbances in supply voltage that may cause damages to the equipment are short- or long-duration overvoltages, switching transients, atmospheric surges and voltage imbalances. The main factors determining the overvoltages are the magnitude, duration, susceptibility, grounding condition and existing protection of the equipment. Measures to reduce the occurrence of damages can be implemented in the supply system or in the installations of customers. Either the measures could reduce the susceptibility of consumers' equipment to supply side faults or they could reduce the probability that internal problems from one consumer affect other consumers. Knowing the place and cause of a problem allows the company to adopt preventive measures towards future problems and therefore helps improving continuity indicators. Usually, there is no information on the causes of temporary faults in the distribution grid. Obtaining reliable information is a task that requires long-duration research work.

Paper [B4-0192(BR)] discusses best practices to reduce damage claims related to power appliances. Disturbances in the distribution grid may lead to damages of equipment and therefore to claims for compensation. However, it does not seem reasonable for utilities to bear all the burden of compensation for damaged equipment. In many cases, the damage could have been prevented if there were stricter requirements to manufacturers regarding the installation of protectors against overvoltages. In various countries, the installation of protection against transient overvoltages has been made compulsory. Where it is not compulsory, the utilities started to offer surge protection device (SPD) installation services. Both, the regulations and the services lead to a clear reduction in the number of cases of burning equipment. In the case of Brazil, there are standards specifying which protections are adequate for cases of overvoltages, lack of voltage, undervoltage and overcurrents.

However, most Brazilian utilities only recommend that their consumers install SPD's and most consumers ignore this recommendation. This paper proposes two ways for improving the protection against transient overvoltages. The utilities could install SPD compulsory in new consumers' inputs and establish a deadline for existing consumers to adapt to the new requirements or they could start to offer SPD installation services. Furthermore, insurance companies should establish by contract compulsory installation of SPDs.

[B4-0193(BR)] focuses on the influence of distributed photovoltaic generation on the supply voltages and on the claims for compensation for electric damages. For this study, several typical distribution grids were defined and implemented in MATLAB to simulate the impacts of distributed PV generation. In total, a sequence of 14 simulations was conducted. The maximum solar panel power was either 3.5 kW or 7.0 kW at two different common coupling points (CCP) between utility and consumer and the solar generation amplitude varied in steps with a first step at the initial instant and a second step at instant 2 s or only a single step at instant 2 s. Fig. B4-16 (a) shows the results in case of an increase and (b) shows the results in case of a decrease in solar irradiation. The red curves correspond to the impact on CCP1 and the black curves correspond to CCP2. In all situations, the values of the voltages in the CCPs never exceeded the established operation limits. Furthermore, the voltage settling times were short, generally in the order of 0.5 s. The results of the simulations show that the solar generation input or output is not expected to cause conditions that lead to damaged equipment and consequently to claims for compensation.

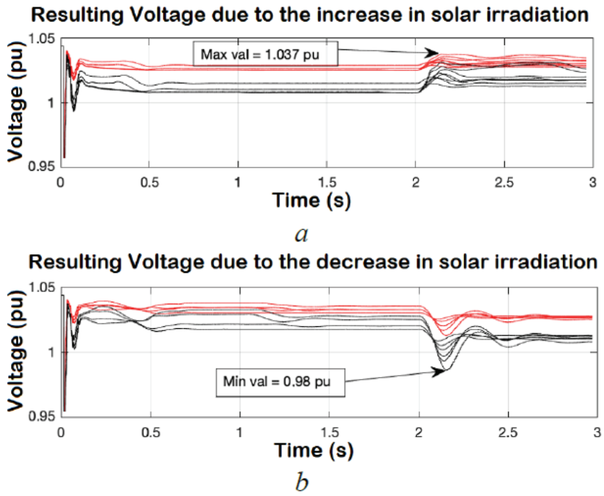

Fig. B4-16: Impact on the CCP voltages with CCP1 voltages (red) and CCP2 voltages (black) in case of an increase (a) or decrease (b) in solar irradiation [B4-0193(BR)]

[B4-0689(DE)] is about the influence of area-structural characteristics on reliability of supply. So far, in quality regulation in Germany only the area-structural characteristic of load-density has been considered. A hyperbolic relationship between the unavailability index ASIDI (MV) or SAIDI (LV) and the load density (LD) has proven to be meaningful:

$$ASIDI_{Ref}(LD)\ or\ SAIDI_{Ref}(LD) = a \cdot {}^{1}/_{LD^{c}} + b.$$

The question arises, if alternative parameters or a combination of several regional structural features could provide stronger explanations. Publicly available high-resolution data are used to map the supply task and the geographical structure. The networks are generated using an algorithm in the form of standard operating resources depending on the supply task. In each case, complete distribution grids are developed that are able to fulfil the given supply task. Stochastic investigations can be carried out based on these grids. Planning principles can be used to map an endogenous specification of a network operator for network design and equipment. All investigations were carried out for ASIDI and for ASIFI parameters.

Area-structural characteristics like load density, connection density, average individual load size over all connections, and generation power density were examined individually to estimate their contribution to differences in supply reliability. Additionally, the industrial or commercial load share as percentage of the total annual peak load was considered. Table 5 shows the parameters of the regression function (ASIDI) and the statistical test results. The regression analysis shows that load density and connection density are the structural characteristics with the highest explanatory contributions. In addition to classical area-structural characteristics, parameters for describing the inhomogeneity of the supply task appear to be useful. To describe this inhomogeneity in the area of low load density, multiple regression is required. The starting point in each case is the load density combined with other characteristics. The contribution of load density for both reliability parameters ASIDI and ASIFI is confirmed for the MV level, if only one characteristic is considered. However, the multiple regression of classical area structural characteristics shows no clear statistical significance for the addition of a parameter to the load density.

Table 5: Parameters of the regression function (ASIDI) and statistical test results (classical area-structural characteristics) [B4-0689(DE)]

parameter	a	b	c	adj. R^2	F-test	t-test
load density	125,6	5,3	0,56	0,60	✓	✓
connection density	14,9	3,7	0,54	0,53	✓	✓
avg. individual load size	1032	3,0	1,12	0,53	✓	✓
generation power density	25,7	0	0,14	0,08	✓	-
industrial + commercial load share	20,5	5,24	-0,88	0,48	✓	✓

The effect of one free disconnection/connection service offered to MV customers to the power grid's outages and inadequate voltage quality parameters are presented and discussed in [B4-0907(PT)]. The reason for this decision is the fact that a relevant percentage of incidents in the MV power grid originate on MV customers' electrical facilities. The main Portuguese DSO has implemented this measure in 2014 and the subsequent evolution of disconnections/connections, the incidents on MV customer installations and their impact on the SAIDI indicator are presented. The results show that the DSO saw a threefold increase in maintenances in customer installations from 2016 to 2020. In the same timeframe, the number of incidents on customer secondary substations decreased by 18%, while their SAIDI contribution decreased by 0.83 minutes This paper concludes that the incentive created to increase the maintenance rate of MV customers was a success in terms of increase of periodic preventive maintenances. Consequently, the number of incidents as well as the SAIDI contribution was reduced. By looking at the cost of the presented measure being on average 200 k€ per year, it is determined that one free disconnection/ connection measure offered to MV customers is a very cost-effective measure compared to the cost of measures for a similar reduction in SAIDI.

Fig. B4-17: Impact of the MV customer incidents on SAIDI indicator (minutes) [B4-0907(PT)]

Potential scope of discussion

Changes in the distribution system are getting faster and faster. With the net zero goals and the green energy pact, these developments will even intensify in the following years. This means also that power quality which is taken for granted in many places will become a hot topic with sensitive apparatus and systems on the one hand and a new mix of emissions on the other hand.

Distribution system operators should therefore monitor power quality constantly in order to identify trends in disturbances and take measures early before a tripping point is reached where large investments need to be undertaken. This applies even more to efforts in standardization and regulation, which also need to anticipate these changes. The goal will always be to enable coordination of emission and compatibility levels for an efficient operation of the distribution grid.

Table 6: Overview of papers in Block 4

Paper (No. and Title)		MS	RIF	PS
0030	Visualizing the Results from unsupervised Deep Learning for the Analysis of Power-Quality Data			I
0049	Spectrum Analysis of Transients using the Short-Time Fourier Transform			I
0065	D-A-CH-CZ Survey on MV Grid Characteristics for the Improvement of Emission Limit-Allocation for large Customer Installations			I
0071	Graphical Methods for presenting time-varying Harmonics			X
0076	Estimation of safe harmonic Hosting Capacity			X
0080	Harmonic Correlations Matrices to present Measurement Results from single and multiple Locations	X		
0085	Mitigation of Inter-Area Power Oscillations in electrical Power System via fuzzy control based Battery Energy Storage Systems			X
0090	Risk Assessment of Server Outages due to Voltage Dips in the internal Power Supply System of a Data Center			I
0160	Deep Learning for Pattern Recognition of Interharmonics in Time-Series and Spectrograms			I
0191	Study of Disturbances in Low Voltage Supply and Proposal of Measures to reduce the Damage of Appliances			X
0192	Recommendations of best Practices to reduce Damage Claims in Power Appliances			X
0193	Evaluation of the Impact of distributed Generation in the Process of Analysis of Damage Claims of electrical Appliances			X
0274	Comparison of Algorithms for Flicker Irritation Assessment	X		X
0370	A View of 2020 Power Quality within GB Distribution Networks	X		
0372	An integrated Platform for Power Quality Monitoring			I
0438	Application of Measurement Methods for the Frequency Range 2-150 kHz to long-term Measurements in public Low Voltage Networks	X		
0575	Harmonic Risk Estimation on LV Networks by Machine Learning	X		
0576	Automatic Identification of Correlations in large Amounts of Power Quality Data from long-term Measurement Campaigns			I
0689	Influence of Area-Structural Characteristics on Reliability of Supply of Electrical Distribution Networks			I
0727	First Steps towards a standardized Hosting Capacity Method			X
0772	Assessment of harmonic Contribution of Customer Installations based on Field Measurements			I
0841	New interharmonic Subgroup Definitions for quantifying and limiting Distortion in Distribution Networks	X		X
0852	Overview of Standards Development within the Power Quality Subcommittee of the IEEE Power & Energy Society			I
0871	Enhanced Machine Learning Methods for nonlinear harmonic Source Modelling			I
0907	Power Quality Impact Analysis of Measures to encourage MV Customers to perform periodic Secondary Substation Maintenances			I
0932	A Comparison of Methods for calculating Harmonic Emission Limits for Customer Installations connected to MV/LV Systems used in Germany and United States			I
0950	High-Order Harmonic Emission in Low Voltage Networks			I
1009	The third Edition of the Austrian-Czech-Swiss-German (D-A-CH-CZ) technical Rule for Assessment of Network Disturbances			I
1031	Presenting a new Correction factor for IEC 60364-5-52 Standard in Cable Calculations under harmonic Conditions			X

1051	Power Quality Monitoring Data Management and Analysis for Distribution Networks			I
1132	Site Indices for High Frequency Harmonics for Long Term Power Quality Monitoring			X
1150	Pre-Normalisation of Grid Impedance Measurement in the Power Line Communication Frequency Band			I

I: interactive poster presentation